

1 **Freeze drying of polyelectrolyte complex nanoparticles: effect of nanoparticle**
2 **composition and cryoprotectant selection**

3

4 Anita Umerska ^{a, b)}, Krzysztof J. Paluch ^{a), c)}, Maria-Jose Santos Martinez ^{d), e)}, Owen I. Corrigan
5 ^{a)}, Carlos Medina ^{d)}, Lidia Tajber ^{a) *}

6

7 a) School of Pharmacy and Pharmaceutical Sciences, Trinity College Dublin, Dublin 2, Ireland.

8 b) Université de Lorraine, CITHEFOR, F-54000 Nancy, France.

9 c) School of Pharmacy and Medical Sciences, Centre for Pharmaceutical Engineering Science,
10 Faculty of Life Sciences, University of Bradford, Richmond Rd., BD71DP, UK.

11 d) School of Pharmacy and Pharmaceutical Sciences & Trinity Biomedical Sciences Institute,
12 Trinity College Dublin, Dublin 2, Ireland.

13 e) School of Medicine, Trinity College Dublin, Dublin 2, Ireland.

14

15 *To whom correspondence should be addressed: lidia.tajber@tcd.ie

16 Phone: 00353 1 896 2787 Fax: 00353 1 896 2810

17

18 **Abstract**

19 This work investigates the impact of nanoparticle (NP) composition and effectiveness of
20 cryo-/lyo-protectants in a freeze drying process, which was employed to convert liquid
21 dispersions of polyelectrolyte complex (PEC) NPs into completely redispersible powders. PEC
22 NPs, with and without peptide, were produced by complex coacervation. The cryo-/lyo-
23 protectants investigated were mannitol, trehalose (TRE) and poly(ethylene glycol) (PEG).
24 The solid state of lyophilised powders was studied by thermal analysis and X-ray diffraction.
25 Cytotoxicity studies were done by MTS assay and flow cytometry. The presence of a
26 cryoprotectant was essential to achieve a successful powder reconstitution. The
27 concentration of TRE was optimised for each type of PEC NPs. Protamine- and hyaluronate-
28 based NPs reconstituted better than chitosan- and chondroitin sulphate-based NPs,
29 respectively. PEG polymers were found to be more effective cryoprotectants than TRE and
30 best results were achieved using co-freeze drying of NPs with TRE and PEG. These ternary
31 NPs/TRE/PEG samples were crystalline, with expected better storage stability. PEG polymers
32 were well tolerated by Caco-2 cells, with the exception of linear PEG 10 kDa. This work
33 shows that, as regards the formulation design and maximising NP loading in the dried
34 product, optimisation of the cryoprotectant type and content is needed as it is highly
35 dependent not only on the type of polyelectrolyte pair in the PEC, but also the polyions
36 ratio.

37

38

39 **KEYWORDS:** polyelectrolyte complex nanoparticle, freeze drying, hyaluronate, chitosan,
40 chondroitin, protamine

41

42 **1. Introduction**

43 Nanoparticles (NPs) have been widely investigated for medical applications such as
44 drug delivery systems and tissue engineering (Shi et al., 2010). A considerable effort is
45 currently being directed towards developing NPs composed of naturally occurring polymers
46 such as polysaccharides, in view of their advantages such as biodegradability, safety, low
47 toxicity, satisfactory stability, abundant resources in nature and low processing costs (Liu et
48 al., 2008). Natural polysaccharides are mainly polyelectrolytes, which present an ionic form
49 in aqueous solutions. These polyelectrolytes can spontaneously associate in complexes and
50 form NPs with substances that bear opposite charge via electrostatic interactions.
51 Polyelectrolyte complex (PEC) NPs can be obtained using complex coacervation, a simple
52 method carried out under mild conditions involving mixing of diluted aqueous solutions of
53 polyelectrolytes at room temperature. This approach at making PEC NPs can prevent
54 destruction of the structure and property of biochemical drugs, if incorporated into NPs,
55 including nucleic acids, peptides and proteins (Cegnar et al., 2011; Yang et al., 2015).
56 Furthermore, complex coacervation does not involve the use of organic solvents and/or
57 surfactants and thus is a very attractive approach at making a wide range of NPs for drug
58 delivery applications.

59 However, NPs, as colloidal systems, are thermodynamically unstable and are
60 susceptible to aggregation after periods of storage as a dispersion. Long term stability is an
61 important challenge in the development of NP formulations, especially systems made of
62 polyelectrolytes (Katas et al., 2013). Freeze drying is an attractive approach to achieve the
63 long term stability of NPs formulations as it requires small sample volumes and is relatively
64 easy to scale up (Boge et al., 2018). Lyophilised formulations provide easy handling including
65 shipping and storage (Lu and Pikal, 2004). Moreover, as solid state dosage forms, such as
66 tablets or capsules, remain the formulations of choice for oral drug delivery, the NPs that
67 are prepared as aqueous dispersions must be transformed into dry powders to be further
68 processed into solid state dosage forms (Wong et al., 2018). It is recognised that stress
69 generated during freeze drying (freezing and water removal) may adversely impact the
70 properties of NPs (Abdelwahed et al., 2006; Fang et al., 2009). Additionally, inadequate
71 reconstitution of freeze dried NPs in the aqueous media represents a major obstacle
72 because it can lead to the formation of large particle aggregates and the loss of beneficial
73 colloidal properties of the nanosystem (Cegnar et al., 2011). Many studies published to date

74 presented that, to effectively stabilise NPs during freeze drying as well as to ensure their
75 adequate reconstitution, suitable excipients are required (de la Fuente et al., 2008; Fang et
76 al., 2009). They typically include using a cryo- and/or lyo-protectant that protects the NPs
77 during the freezing and/or drying stage of the process, respectively.

78 Although lyophilisation of various types of NPs have been studied (Abdelwahed et
79 al., 2006), optimal conditions depend mainly on the nature of particle systems, thus have to
80 be customised for each formulation (Cegnar et al., 2011). Freeze drying of polyelectrolyte
81 complex NPs presents a particular challenge, as they are mainly stabilised by charge, thus
82 susceptible to changes in the medium parameters (pH and ionic strength) (Cegnar et al.,
83 2011), their shape/structure is less defined (Umerska et al., 2014b) as opposed to e.g.
84 poly(lactic-co-glycolic) acid-based NPs and are surfactant-free formulations and surfactants
85 such as polyvinyl alcohol can act as cryo-/lyo-protectants and facilitate redispersibility of the
86 NPs (Umerska et al., 2018). For PEC NPs, freeze drying of chitosan-based NPs has been
87 studied (Rampino et al., 2013), including alginate/chitosan (Cegnar et al., 2011) and
88 hyaluronate-coated chitosan NPs (Veilleux et al., 2018), but not other types of PEC NPs.
89 Thus, there is a literature gap as the main focus of research is often formulate NPs with a
90 specific delivery target but not on subsequent transformation into the solid state for long-
91 term stability. For instance, de la Fuente et al. (2008) freeze dried only one type of
92 polyelectrolyte hyaluronate-chitosan-tripolyphosphate NPs (concentration range between
93 0.075 and 0.5 mg/ml) in the presence of either glucose or trehalose at a relatively high
94 concentration of 5% w/v, but freeze drying was not the main subject of the study and no
95 deep investigation into this subject was performed such as effective minimising of
96 cryoprotectant concentration or influence of the NP composition.

97 The addition of a suitable lyo-/cryo-protective agent before freezing prevents NPs
98 from aggregating. It is well established that sugars can be employed for this purpose (Boge
99 et al., 2018; Cegnar et al., 2011; Rampino et al., 2013). Non-reducing compounds such as
100 trehalose, mannitol and sucrose are preferred to avoid potential Maillard reaction of the
101 excipient with protein, especially for protein-based nano-formulations (Anhorn et al., 2008).
102 Those compounds have been shown to be effective in maintaining the properties of NPs
103 after the lyophilisation process (Anhorn et al., 2008; Holzer et al., 2009). The advantages of
104 trehalose over other sugars include lower hygroscopicity, the absence of internal hydrogen
105 bonds and consequently more flexible formation of hydrogen bonds with NPs, a very low

106 chemical reactivity and, finally, a high glass transition temperature (Abdelwahed et al.,
107 2006; Crowe et al., 1996; Hafner et al., 2011). Apart from trehalose, poly(ethylene glycol)
108 (PEG) polymers have also been used as stabilisers in freeze drying of NPs including chitosan
109 NPs (Rampino et al., 2013), however no systematic study on the influence of molecular
110 weight or branching has been published thus far.

111 In this work, two polycations, chitosan (CHIT) and protamine (PROT), and two
112 polyanions, hyaluronic acid (HA) and chondroitin sulphate (CHON), were examined as
113 candidate components of PEC NPs. These polyelectrolytes possess numerous advantages as
114 they are reasonably cheap, biocompatible, biodegradable, of natural origin, already well
115 characterised and have history of use in pharmaceutical products. They have received a
116 particular attention as carrier materials because they present interesting biological and/or
117 pharmacological properties. CHON exhibits anti-inflammatory activity (Iovu et al., 2008) and
118 is currently used as a chondroprotective drug together with glucosamine. HA also exhibits
119 anti-inflammatory effects (Ryan et al., 2013) and binds to the CD44 receptor, which is
120 overexpressed in a wide variety of cancer cells and therefore has been extensively studied
121 as a therapeutic target (Platt and Szoka, 2008). Moreover, HA coating considerably reduces
122 hemolysis and hemagglutination of chitosan polyplexes and thereby facilitates intravenous
123 administration (Veilleux et al., 2018). CHIT has antibacterial activities (Raafat et al., 2008),
124 while PROT is used as an antagonist for heparin (Jaques, 1973) and due to the presence of
125 arginine it provides membrane translocation activities (Reynolds et al., 2005).

126 Considering the above, the goal of this work is to identify if and how the type of a
127 lyo-/cryo- protective agent, its concentration and composition of NPs (type, starting
128 concentration and content of polyions as well as the presence of a peptide) affect the ability
129 of liquid NP dispersions to be freeze dried into powders that completely redisperse upon
130 reconstitution. The solid state of lyophilised products was examined as the
131 amorphous/crystalline character of the powder may determine the storage shelf-life, while
132 the cytotoxic properties may limit the use of some of the excipients from wider applications.

133 **2. Materials and methods**

134 **2.1. Materials**

135 Hyaluronic acid sodium salt (HA) from *Streptococcus equi* sp. (sodium content 3.6%
136 w/w, molecular weight app. 2900 kDa), chondroitin 4-sulfate sodium salt (CHON, sodium
137 content 5.6% w/w, molecular weight 59 kDa), protamine sulphate (PROT, molecular weight

138 5.1 kDa), trehalose dihydrate and poly(ethylene glycol) (PEG) linear polymers with different
139 molecular weights were purchased from Sigma-Aldrich (Ireland). Chitosan chloride high
140 molecular weight (CHH, chloride content 15.5% w/w, degree of deacetylation 83%,
141 molecular weight 110 kDa) was obtained from Novamatrix (Norway), while chitosan chloride
142 low molecular weight (CHL, chloride content 13.6% w/w, degree of deacetylation 82%,
143 molecular weight 42kDa) was acquired from Chitoceuticals (Germany). Four-arm branched
144 PEG with a molecular weight of 10 kDa was sourced from JenKem Technology USA Inc.
145 (Allen, USA). Salmon calcitonin (sCT) was obtained from PolyPeptide Laboratories (Sweden).
146 APC annexin V and propidium iodide were purchased from BD Biosciences (USA) and
147 CellTiter 96® Non-Radioactive Cell Proliferation Assay from Promega Corporation (USA).
148 Other cell culture reagents were provided by Sigma Aldrich (Ireland). All other reagents,
149 chemicals and solvents were of analytical grade.

150 **2.2. Methods**

151 **2.2.1 Preparation of polyelectrolyte NPs**

152 All NPs were synthesised using a surfactant- and solvent-free polyelectrolyte complexation
153 in an aqueous media as previously described (Umerska et al., 2017, 2015, 2014b, 2012).
154 Briefly, all solutions of polyions were made in deionised water. HA solutions were sonicated
155 before mixing with a polycation solution for 2 hours at an amplitude of 80% (13 W) with the
156 aid of a 130 Watt ultrasonic processor (SONICS VC130PB, Sonics and Materials Inc., USA) to
157 obtain HA fragments with a molecular weight of app. 260 kDa.

158 Chitosan-based NPs (CCH or CHL) were made using either 1 or 2 mg/ml solutions of the
159 polycation. A volume of the chitosan solution was added to a predefined volume of the
160 polyanion solution, HA or CHON at 1 or 2 mg/ml, using a one shot addition at room
161 temperature under magnetic stirring. The stirring was maintained for 10 minutes to allow
162 stabilisation of the system. Details of composition, including the total polyion concentration
163 (TPC) and the polyanion to polycation mass mixing ratio (MMR) of the various systems made
164 are summarised in Table 1.

165 PROT-based systems were made as follows. An aliquot of 4 ml of PROT aqueous solution
166 with various concentrations, as outlined in Table 2, was added to 10 ml of a HA or CHON
167 solution at room temperature under magnetic stirring. The stirring was maintained for 10
168 minutes to allow stabilisation of the system, as for the chitosan-based NPs.

169 To make salmon calcitonin-containing NPs, the peptide was dissolved at a concentration of
 170 0.5 mg/ml in the HA or CHON solution and mixed with a solution of the polycation as
 171 described above.

172

173 **Table 1** Composition and characteristics of chitosan-based NPs. The PS, PDI and ZP values
 174 were measured directly after manufacturing the NP systems, before cryoprotectant addition
 175 and freeze drying. HA – hyaluronic acid, CHON – chondroitin sulphate, CHH – chitosan high
 176 molecular weight, CHL - chitosan low molecular weight, PA – polyanion, PC- polycation,
 177 MMR - PA/PC mass mixing ratio, TPC – total polyelectrolyte concentration, sCT – salmon
 178 calcitonin, PS - hydrodynamic particle size, PDI – polydispersity index and ZP – zeta
 179 potential.

NP system	PA	PC	MMR	TPC (mg/ml)	sCT conc. (mg/ml)	PS (nm)	PDI	ZP (mV)
HA/CHH _{1;1}	HA	CHH	1	1	0	260	0.19	+53
HA/CHH _{1;2}	HA	CHH	1	2	0	403	0.44	+64
HA/CHH _{2.5;1}	HA	CHH	2.5	1	0	172	0.11	-36
HA/CHH _{2.5;2}	HA	CHH	2.5	2	0	235	0.21	-42
HA/CHH _{5;1}	HA	CHH	5	1	0	218	0.21	-63
HA/CHH _{5;2}	HA	CHH	5	2	0	255	0.28	-87
HA/CHH _{5;1} sCT	HA	CHH	5	1	0.5	161	0.08	-30
CHON/CHL _{1;1}	CHON	CHL	1	1	0	96	0.13	+35
CHON/CHL _{1;2}	CHON	CHL	1	2	0	128	0.12	+35
CHON/CHL _{2.5;1}	CHON	CHL	2.5	1	0	78	0.14	-46
CHON/CHL _{2.5;2}	CHON	CHL	2.5	2	0	100	0.12	-44
CHON/CHL _{5;1}	CHON	CHL	5	2	0	85	0.17	-54
CHON/CHL _{5;2}	CHON	CHL	5	1	0	90	0.24	-53
CHON/CHL _{5;1} sCT	CHON	CHL	5	1	0.5	95	0.22	-44

180

181 **Table 2** Composition and characteristics of PROT-based NPs. The PS, PDI and ZP values were
 182 measured directly after manufacturing the NP systems, before cryoprotectant addition and
 183 freeze drying. HA – hyaluronic acid, CHON – chondroitin sulphate, PROT – protamine, PA –
 184 polyanion, PC- polycation, MMR - PA/PC mass mixing ratio, TPC – total polyelectrolyte
 185 concentration, sCT – salmon calcitonin, PS - hydrodynamic particle size, PDI – polydispersity
 186 index and ZP – zeta potential.

NP system	PA	PA conc. (mg/ml)	PC	PC conc. (mg/ml)	MMR	TPC (mg/ml)	sCT conc. (mg/ml)	PS (nm)	PDI	ZP (mV)
HA/PROT _{2.1;low}	HA	0.714	PROT	0.343	2.1	1.06	0	159	0.11	-39
HA/PROT _{3.1;low}	HA	0.714	PROT	0.229	3.1	0.94	0	119	0.14	-51
HA/PROT _{6.3;low}	HA	0.714	PROT	0.114	6.3	0.83	0	87	0.20	-69
HA/PROT _{6.3;low} sCT	HA	0.714	PROT	0.114	6.3	0.83	0.5	140	0.20	-39
HA/PROT _{3.1;high}	HA	1.429	PROT	0.457	3.1	1.89	0	159	0.14	-57
HA/PROT _{6.3;high}	HA	1.429	PROT	0.229	6.3	1.66	0	127	0.17	-94
HA/PROT _{12.5;high}	HA	1.429	PROT	0.114	12.5	1.54	0	107	0.20	-125
CHON/PROT _{2.1;low}	CHON	0.714	PROT	0.343	2.1	1.06	0	93	0.12	-49
CHON/PROT _{3.1;low}	CHON	0.714	PROT	0.229	3.1	0.94	0	78	0.15	-52

CHON/PROT _{6.3;low}	CHON	0.714	PROT	0.114	6.3	0.83	0	88	0.40	-57
CHON/PROT _{6.3;low} SCT	CHON	0.714	PROT	0.114	6.3	0.83	0.5	61	0.42	-43
CHON/PROT _{3.1;high}	CHON	1.429	PROT	0.457	3.1	1.89	0	78	0.16	-50
CHON/PROT _{6.3;high}	CHON	1.429	PROT	0.229	6.3	1.66	0	84	0.26	-54
CHON/PROT _{12.5;high}	CHON	1.429	PROT	0.114	12.5	1.54	0	88	0.40	-59

187

188 **2.2.2 Freeze drying and redispersibility of NPs**

189 An appropriate amount of trehalose dihydrate (TRE), poly(ethylene glycol) (PEG, with
190 molecular weight of 2,000 or 4,000 or 10,000 linear or 10,000 branched) or a mixture of TRE
191 and PEG was added to NP dispersion and dissolved. The concentrations of TRE presented in
192 this work refer to trehalose dihydrate. The ratios of anhydrous trehalose to NP in
193 weight/weight ratios are presented in Figure 1.

194 Aliquots of the formulation (4 ml) were dispensed into 15 ml Greiner plastic
195 centrifuge tubes and immediately shock-frozen in liquid nitrogen (Abdelwahed et al., 2006;
196 Molpeceres et al., 1997). Tubes with the frozen samples were placed in VirTis wide mouth
197 filter seal glass flasks and attached to one of the ports of manifold of a benchtop VirTis 6K
198 freeze dryer model EL (SP Scientific, USA). Vacuum of 29-31 mtorr was obtained by the use
199 of an Edwards 5 RV5 rotary vane dual stage mechanical vacuum pump (Edwards, England).
200 After 48 hours of freeze drying the tubes were removed, capped and stored at 4 °C if
201 storage was required. Freeze drying was performed on at least three independent samples
202 of each formulation.

203 Sample reconstitution was performed by adding 4 ml of water (or serum-free
204 medium for cell culture experiments) to the whole content of powder in the 15 ml tube and
205 manual, moderate shaking. No sonication or mechanically-assisted mixing was employed.
206 Samples after reconstitution were analysed in triplicate.

207 **2.2.3 Particle size and zeta potential analysis**

208 The intensity-averaged mean particle size (particle size diameter) and the
209 polydispersity index of the nanoparticles were determined by Dynamic Light Scattering (DLS)
210 with the use of 173° backscatter detection and the electrophoretic mobility values
211 measured by Laser Doppler Velocimetry (LDV) were converted to zeta potential by the
212 Smoluchowski equation, as described before (Umerska et al., 2012). DLS and LDV
213 measurements were done using a Zetasizer Nano series Nano-ZS ZEN3600 fitted with a 633
214 nm laser (Malvern Instruments Ltd., UK). Samples were placed directly into the folded

215 capillary cells (DTS1061) without dilutions. Each analysis was carried out at 25 °C with the
216 equilibration time set to 5 minutes. The readings were carried out at least three times for
217 each batch and the average values of at least three batches are presented. The results were
218 adjusted taking into account viscosity of the continuous medium.

219 For the clarity of data presentation and discussion, hydrodynamic particle size (PS)
220 ratios were calculated for all NP systems, defined as the ratio of the size after and before
221 freeze drying. The redispersibility was considered as very good, when the particle size did
222 not change more than 20% (i.e. the PS ratio was between 0.8-1.2). For comparison, Fang et
223 al. (2009) considered the ratio of 0.7-1.3 ($\pm 30\%$) appropriate, indicating satisfactory
224 reconstitution.

225 **2.2.4 Separation of non-associated sCT and quantification of the peptide**

226 Non-associated sCT was separated from nanoparticles by a combined ultrafiltration-
227 centrifugation technique (Centriplus YM-50, MWCO of 50 kDa for HA-based NPs or Amicon
228 Ultra-15, MWCO of 30 kDa for CHON-based NPs; Millipore, USA) using a validated technique
229 as described before (Umerska et al., 2015, 2014b, 2014a). The quantity of total and non-
230 associated sCT was measured by an isocratic HPLC method presented previously (Umerska
231 et al., 2014b). Association efficiency (AE) and sCT loading (PL) were calculated with the use
232 of the following equations:

$$233 \text{AE} = [(A-B)/A] * 100\% \quad (\text{Eqn. 1})$$

234 where A is the total amount of sCT and B is the mass of non-associated sCT;

$$235 \text{PL} = [(A-B)/C] * 100\% \quad (\text{Eqn. 2})$$

236 where C is the total weight of all the components of NPs.

237 **2.2.5 Differential Scanning Calorimetry (DSC)**

238 DSC experiments were conducted using a Mettler Toledo DSC 821^e with a
239 refrigerated cooling system (LabPlant RP-100, UK), according to the method presented by
240 Umerska et al. (2015). Nitrogen was used as the purge gas. Hermetically sealed aluminium
241 pans with three vent holes were used throughout the study and sample weights varied
242 between 2 and 7 mg, depending on bulk density of the sample. DSC measurements were
243 carried out at a heating/cooling rate of 10 °C/min.

244 **2.2.6 Powder X-ray diffraction (PXRD)**

245 Powder X-ray diffraction analysis was conducted using a Rigaku Miniflex II desktop X-
246 ray diffractometer (Rigaku, Japan) operating at 30 kV and 15 mA and fitted with a Haskris

247 cooling unit. Ni-filtered Cu K α radiation ($\lambda=1.5408 \text{ \AA}$) was used. Room temperature
248 measurements were recorded for the range 5-40 2theta degrees at a step size of 0.05° per
249 second. A low background silicon mount (Rigaku, Japan) was used to support the sample
250 during measurements.

251 **2.2.7 Cell culture studies**

252 Human epithelial colorectal adenocarcinoma cells (Caco-2) were obtained from
253 European Collection of Cell Cultures (Sigma-Aldrich, UK). Cells were cultured in 75 cm² cell
254 culture flasks in Eagle's Minimal Essential Medium (MEM), supplemented with 20% foetal
255 bovine serum, penicillin (0.006 mg/ml), streptomycin (0.01 mg/ml), gentamicin (0.005
256 mg/ml), sodium bicarbonate (2.2 g/l), sodium pyruvate (0.11 g/l), pH 7.4 at 5% CO₂ and 37
257 °C humidified atmosphere (CO₂ incubator series 8000DH, ThermoScientific). Cells were
258 supplied with fresh medium every second day and split after detaching with
259 ethylenediaminetetraacetic acid (EDTA)-trypsin twice a week. For experimental purposes
260 the passage number range was maintained between 20 and 30.

261 **2.2.8 MTS assay**

262 MTS assay was carried out according to the method presented previously (Umerska
263 et al., 2015). Briefly, Caco-2 cells were seeded into flat-bottom 96-well plates in 100 μ l of
264 whole media (MEM supplemented with 20% FBS) at a density of 25,000 cells per well (cells
265 were previously counted with the aid of Z1 Coulter Particle Counter, Beckman Coulter) and
266 incubated at 37 °C for 24h. The medium was then replaced with 100 μ l of the sample
267 dispersed or dissolved in serum-free media. After 72 h of incubation, or 24 h when a serum-
268 free medium at pH-5 was used, the supernatant was removed from the wells and replaced
269 with serum-free media. A quantity of 20 μ l of the MTS reagent prepared according to the
270 manufacturer protocol was then added into each well; in case of positive control (0%
271 viability) the media was replaced by 10% SDS solution in serum-free media 30 min before
272 the addition of MTS reagent. After 4 hours the UV absorbance of the formazan product was
273 measured spectrophotometrically (FLUOstar Optima microplate reader, BMG Labtech) at
274 492 nm. Positive control was treated as a blank and its absorbance was subtracted from
275 each reading. The cells viability was expressed as the ratio of the absorbance reading of the
276 cells treated with different samples and for negative control (cells treated with serum-free
277 MEM), which was assumed to have 100% of the cells viability. IC₅₀ values (concentrations
278 required to reduce the viability of cells by 50% as compared with the control cells) were

279 calculated by fitting the experimental points to the Hill equation (Goutelle et al., 2008). At
280 least three different batches of samples were tested in cells with at least three different
281 passage numbers.

282 **2.2.9 Flow cytometry**

283 The content of one 75 cm² flask of confluent Caco-2 cells was seeded into eight 25
284 cm² flasks, each containing Caco-2 cells suspended in 4 ml of MEM supplemented with 20%
285 FBS. Cells were allowed to attach for 24-48 hours. The medium was then replaced with 3 ml
286 of sample (sonicated HA). After 72 hours of incubation the supernatant was removed and
287 cells were harvested with trypsin/EDTA. After neutralisation, the cells were combined with
288 the previously removed supernatant and centrifuged (300 g, 5 minutes); the supernatant
289 from centrifugation was discarded, and cells were washed with binding buffer (0.14M NaCl,
290 0.0025M CaCl₂ and 0.01M 4-(2-hydroxyethyl)-1-piperazineethanesulfonic acid (HEPES), pH
291 7.4 adjusted with NaOH solution). 20 µl of the cells suspension were stained with 5µl of
292 APC-Annexin V, 5 µl of propidium iodide and diluted with 70 µl of binding buffer and
293 incubated in dark at room temperature for 15 minutes. Then the cell suspension was further
294 diluted with binding buffer, transferred to a flat bottom 96-wells plate and applied to flow
295 cytometric analysis. All analyses were performed by a BD FACSArray™ bioanalyser (Becton
296 Dickinson, UK). The instrument was set up to measure the size (forward scatter), granularity
297 (side scatter) and cell fluorescence. Antibody binding was measured by analysing individual
298 cells for fluorescence. The mean fluorescence intensity was determined after correction for
299 cell autofluorescence. Fluorescence histograms were obtained for 10000 individual events.
300 Data were analysed using BD FACSArray™ system software and expressed as a percentage
301 of control fluorescence in arbitrary units. At least three different batches of samples were
302 tested in cells with at least three different passage numbers.

303 **2.2.10 Statistical analysis**

304 The data were analysed using one-way analysis of variance (Minitab software). The results
305 are expressed as mean ± S.E.M. of at least three independent experiments. Tukey-Kramer
306 multiple comparisons test was performed where appropriate. Statistical significance was
307 considered when p<0.05.

308 **3. Results and Discussion**

309 **3.1. Properties of polyelectrolyte complex NPs**

310 Polyelectrolyte complex nanoparticles (PEC NPs) were prepared by a complex
311 coacervation method based on previous reports (Umerska et al., 2017, 2015, 2014a, 2014b,
312 2012). Considering that a very wide range of particles were synthesised and presented in
313 those reports, only formulations that yielded colloiddally stable NPs as well as characterised
314 by small size and large absolute value of zeta potential were selected for the current study
315 and the PEC formation was conducted in diluted solutions to prevent aggregation caused by
316 viscosity of the polyion solutions (Quiñones et al., 2018). Both, positively and negatively
317 charged CHIT NPs were successfully obtained (Table 1). The main factor that determined the
318 zeta potential was the polyanion to polycation mass mixing ratio (MMR) for both, HA/CHIT
319 and CHON/CHIT NPs. The MMR also affected the size and size distribution of these PEC NPs.
320 As it was impossible to obtain physically stable for at least 24 hours PROT NPs, only
321 negatively charged PROT NPs were selected for the lyophilisation studies. The instability of
322 positively charged PROT NPs was attributed to a large difference in molecular weight
323 between PROT and polyanions (either HA or CHON) (Umerska et al., 2014b). Other
324 parameters that affected the properties of obtained PEC NPs were the type of polymer used
325 (HA versus CHON), polymer concentration and incorporation of the peptide.

326 **3.2. Freeze drying and NP reconstitution**

327 **3.2.1. Freeze drying of NPs without a cryoprotectant**

328 Given the fact that HA has been described as an efficient cryoprotectant for freeze
329 drying of liposome formulations (Peer et al., 2003), first attempts at processing were made
330 using native HA/CHH NPs (HA/CHH_{2.5;1} and HA/CHH_{5;1}) dispersions without addition of any
331 protective agents. NPs processed in this way did not redisperse and in the reconstituted
332 suspension aggregates as well as NPs with the average size of a 3-fold greater (HA/CHH_{2.5;1})
333 than the non-processed NPs were present. Similar to this outcome, unsuccessful trials to
334 freeze dry HA-CHIT-tripolyphosphate NPs were made by de la Fuente et al. (2008), who
335 attributed this failure to the presence of only a small amount of HA in the suspending
336 medium after the formation of NPs.

337 The stability of PEC NPs in aqueous dispersions is mainly governed by electrostatic
338 (charge) but also steric (due to the polymeric corona) stabilisation effects. Electrostatic
339 stabilisation is the result of the presence of electrical double layers, which cause particle
340 repulsion, and is determined by the magnitude of the surface or zeta potential, electrolyte
341 concentration and valence (Tadros, 2010). As mentioned earlier, the formation of PEC NPs

342 must be conducted in diluted dispersions to prevent their aggregation. During the freezing
343 step, as a result of ice formation, the liquid phase becomes more concentrated and the
344 distance between the particles decrease, thus increasing interparticulate attraction leading
345 to aggregation. Moreover, the polyelectrolytes are present as salts and the dispersions
346 contain either chloride or sulphate anions from CHIT and PROT, respectively, and sodium
347 cations from either CHON or HA. Although in the initial dispersion the concentration of
348 inorganic counterions is low, the formation of concentrated cryo-solution during the
349 freezing step can markedly increase their concentration, thereby reducing electrostatic
350 repulsion forces (through charge screening).

351 **3.2.2. Freeze drying of polyelectrolyte NPs with mannitol**

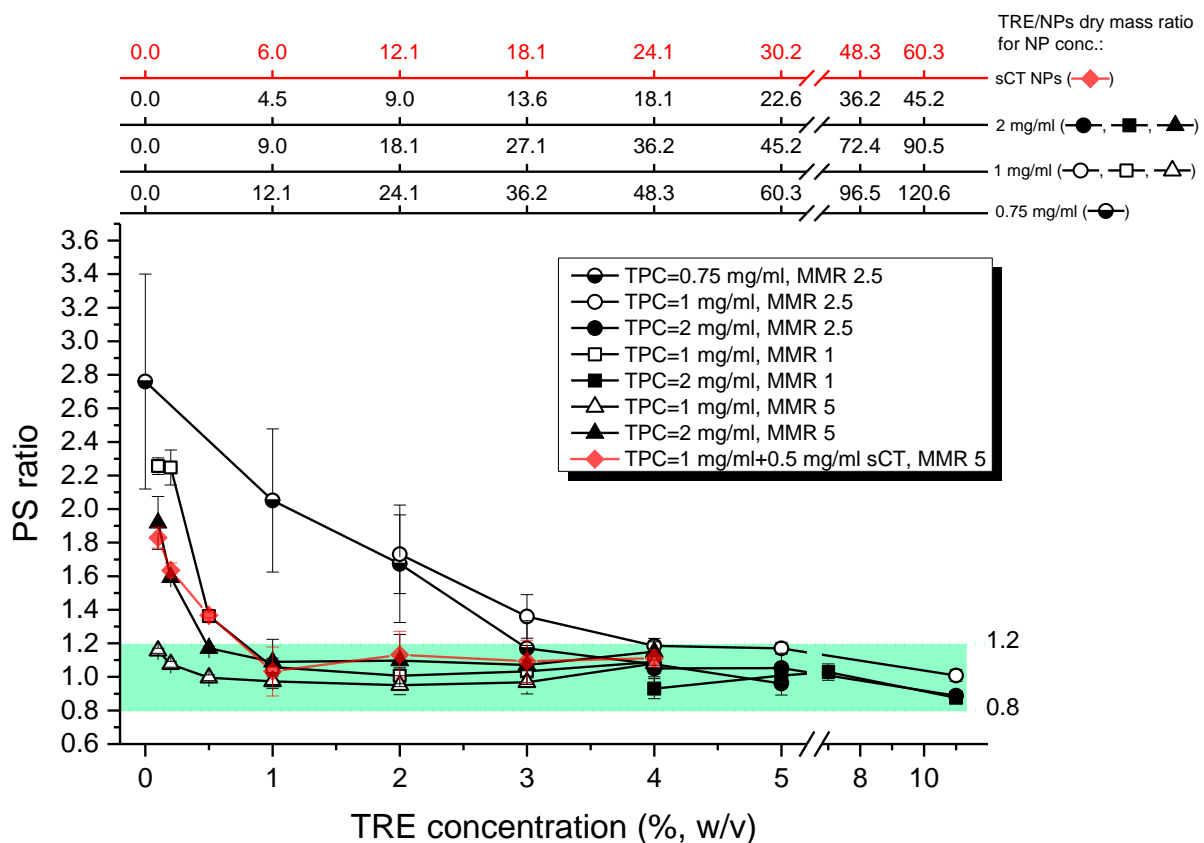
352 Although Anhorn et al. (2008) demonstrated that mannitol can be an effective
353 cryoprotectant for human serum albumin-based NPs, attempts to use mannitol (at 1, 2, 3
354 and 5% w/v) as a cryoprotectant for HA/CHH NPs (HA/CHH_{2.5;1}) were unsuccessful. When
355 HA/CHH NPs were lyophilised with mannitol, a substantial NP coagulation and/or
356 aggregation into microparticles upon reconstitution was seen in all samples tested.
357 Mannitol is a low molecular weight sugar alcohol, which forms a crystalline phase upon
358 lyophilisation (Kim et al., 1998). It is probable that the growing crystals of mannitol induced
359 mechanical stress and resulted in the reduction of space available for NPs. NPs in this
360 nanoparticle-rich and poorly hydrated phase may more readily interact and form aggregates
361 (Abdelwahed et al., 2006; Cegnar et al., 2011; Cesàro et al., 2008; Rampino et al., 2013).
362 Therefore, to achieve an effective preservation of NP properties and successful
363 reconstitution, it appears important that at least a fraction of the cryo-protectant remains
364 molecularly disordered to stabilise the PEC NPs.

365 **3.2.3. Freeze drying of polyelectrolyte NPs with trehalose**

366 **3.2.3.1. HA/chitosan NPs**

367 As it was impossible to successfully redisperse the NPs when freeze dried on their
368 own or with addition of mannitol, preliminary experiments were first conducted to test if
369 trehalose (TRE) could be a viable cryoprotectant for HA/CHH NPs. HA/CHH_{2.5;0.75} and
370 HA/CHH_{2.5;1} were freeze dried in the presence of different concentrations of TRE and the PS
371 ratios are presented in Figure 1. When NPs (HA/CHH_{2.5;0.75}) were lyophilised with 1% w/v
372 TRE, the PS ratio did not change significantly in comparison to HA/CHH_{2.5;1} processed with
373 no cryoprotectant and moderate particle aggregation was observed (Figure 1). An increase

374 in TRE concentration to 2% w/v resulted in a decrease in the PS ratio to 1.67 ± 0.35 and
 375 1.73 ± 0.23 (for HA/CHH_{2.5;0.75} and HA/CHH_{2.5;1}, respectively) and, more importantly, only in a
 376 slight NP aggregation. A very good redispersibility was achieved when HA/CHH NPs were
 377 freeze dried at the TPC of 0.75 mg/ml with 3, 4 or 5% w/v of TRE, as the PS ratio was
 378 between 1.17 ± 0.16 (3% w/v TRE) and 0.96 ± 0.07 (5% w/v TRE) and aggregation was not
 379 seen. However, when the TPC was increased to 1 mg/ml, 3% w/v of TRE produced an
 380 acceptable redispersion and no aggregation was observed, but the particle size increased by
 381 36% after freeze drying in comparison to the starting value.

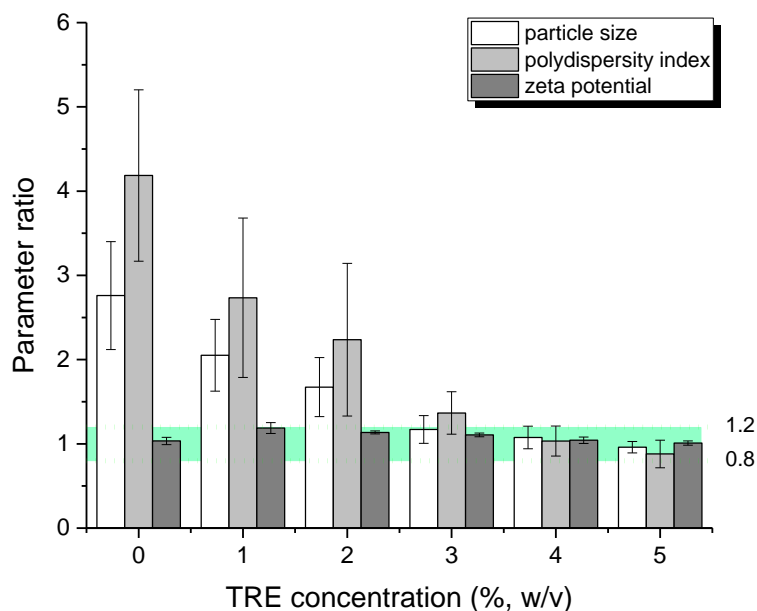


382
 383 **Figure 1.** The particle size (PS) ratio (i.e. the ratio of PS after and before freeze drying) of
 384 HA/CHH NPs freeze dried with trehalose (TRE) at different concentrations. The NP TPC of
 385 0.75 mg/ml was obtained by dilution of 1 mg/ml TPC nanodispersions with TRE solution.
 386 Upper axes present the equivalent TRE (as anhydrous sugar)/NPs dry mass ratio depending
 387 on the concentration of NP components. The green band indicates the PS ratio between 0.8
 388 and 1.2, considered as very good redispersibility of processed NPs. TPC - total
 389 polyelectrolyte concentration, MMR - polyanion/polycation mass mixing ratio, sCT- salmon
 390 calcitonin.

392 The redispersibility of HA/CHH_{2.5;1} was considered to be very good when at least 4%
 393 w/v of TRE was used as the cryoprotectant. When the TPC was further increased to 2 mg/ml
 394 (HA/CHH_{2.5;2}), a significant aggregation was observed and the particles did not fully

395 redisperse even though the size of the particles remaining in non-aggregated fraction did
 396 not change when compared to the PS before lyophilisation (the PS ratio was 1.07 ± 0.05).
 397 When 5% w/v TRE was employed, neither the change of the particle size, nor aggregation
 398 could be observed, therefore at 5% w/v TRE act as an effective cryoprotectant for
 399 HA/CHH_{2.5;2}. Interestingly, when 11% w/v TRE was used in freeze drying, the particle size of
 400 HA/CHH_{2.5;2} became smaller than before lyophilisation (the PS ratio was 0.89 ± 0.02).
 401 However, this decrease in the particle size did not occur when the same sugar concentration
 402 was used to freeze dry HA/CHH_{2.5;1}. The decrease in PS could be attributed to the
 403 compaction of the NP structure (de la Fuente et al., 2008).

404 An example how other properties of NPs (PDI and ZP), in addition to the PS, changed
 405 upon processing with a different concentration of TRE, is shown in Figure 2 for
 406 HA/CHH_{2.5;0.75}. The changes in DPI values were similar to the changes in PS and the ratios of
 407 PS after and before freeze drying did not differ significantly from the equivalent ratios for
 408 PDI. The ZP ratios were seen unaffected by the processing and they remained in the 0.8-1.2
 409 range. Therefore from now on, only changes in relations to the particle size will be
 410 discussed.



411
 412 **Figure 2.** Parameter ratios of: particle size, polydispersity index and zeta potential after and
 413 before processing of HA/CHH_{2.5;0.75} freeze dried with different concentrations of TRE. The
 414 green band indicates the PS ratio between 0.8 and 1.2, considered as very good
 415 redispersibility of processed NPs.
 416

417 As shown previously (Umerska et al., 2012), the composition of NPs, especially the
418 MMR of the polymers has a significant influence on their physical (i.e. PS, PDI and ZP) and
419 biological properties. Therefore the next step in this study was to assess how the NP
420 composition affected their redispersibility after freeze drying.

421 HA/CHH NPs with MMRs of 1 (containing more chitosan, positively charged) and 5
422 (containing more HA, negatively charged) were initially freeze dried at TPCs of 1 or 2 mg/ml
423 with 4% w/v TRE and depending on if the powder redispersed, the concentration of TRE was
424 further increased or decreased to determine the lowest concentration at which good
425 redispersibility could be obtained.

426 Figure 1 illustrates the PS ratios before and after freeze drying of positively charged
427 NPs (MMR = 1). When the TPC was 2 mg/ml (HA/CHH_{1;2}), a significant aggregation was
428 observed with 4% w/v TRE, but the PS ratio was satisfactory (0.93±0.06). Therefore the
429 concentration of sugar was further increased and a successful reconstitution without
430 aggregation could be seen at 5, 7 or 11% w/v of this cryoprotectant, with the PS ratios close
431 to 1 for 5 and 7% w/v of TRE and a significant decrease in the particle size after freeze drying
432 when 11% w/v of TRE was employed. On the other hand, the system with a TPC of 1 mg/ml
433 (HA/CHH_{1;1}) successfully reconstituted after freeze drying with 4% w/v TRE, with a low size
434 ratio (1.09±0.06) and no aggregation observed. The redispersibility remained very good
435 even when 1% w/v TRE was used for this system and when the concentration of TRE was
436 further decreased to 0.5% w/v, a moderate aggregation occurred accompanied by an
437 increase in the particle size by 36%. When the concentration of TRE was again decreased to
438 0.2 or 0.1% w/v, a significant aggregation and a 2.3-fold increase in the PS were observed.

439 HA/CHH NPs with the MMR of 5 were satisfactory redispersible at both TPCs (1 and 2
440 mg/ml, systems HA/CHH_{5;1} and HA/CHH_{5;2}) when 4% w/v TRE was used. No aggregation was
441 observed apart from HA/CHH_{5;2} freeze dried with 0.1% w/v TRE (Figure 1). HA/CHH_{5;1} had a
442 very good redispersibility even after lyophilisation with only 0.1% w/v TRE. The properties of
443 HA/CHH_{5;2} were satisfactorily preserved at TRE concentration down to 0.5% w/v and at TRE
444 0.2% w/v a significant increase in the particle size after the process was observed (the PS
445 ratio was 1.59±0.01). It can therefore be concluded that HA/CHH NPs with the MMR of 5 are
446 characterised by better redispersibility than NPs with MMRs of 2.5 and 1. This may be
447 explained by a markedly higher content of HA in these systems, supporting the finding of
448 Peer et al. (2003) that HA can assist in efficient lyophilisation. Also, the corona in HA/CHH₅

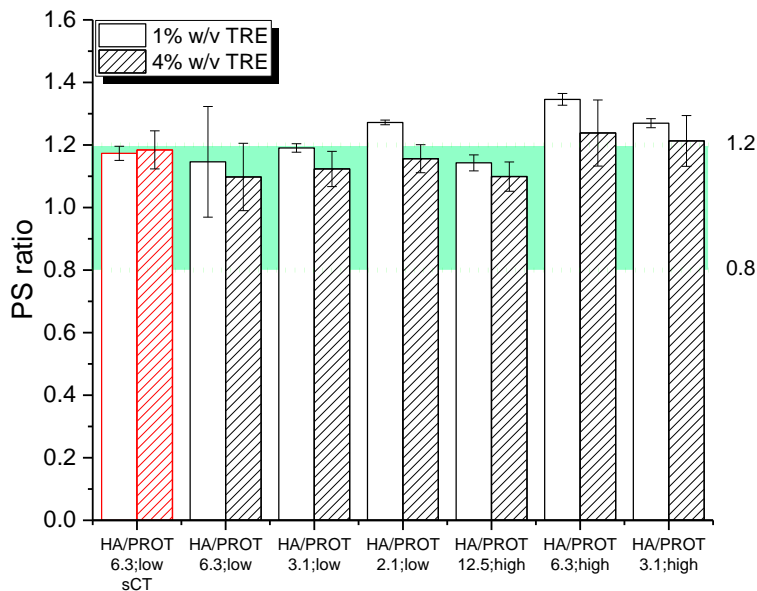
449 NPs is relatively larger than in the HA/CHH_{2.5} system, the latter being composed
450 predominantly of a dense core (Umerska et al., 2012). As the corona is characterised by a
451 smaller density than the core, it is possible that the molecules of a cryoprotectant penetrate
452 inside the corona in spaces between HA chains, therefore enabling better preservation of
453 particle properties during exposure to stress associated with the freeze drying process.

454 The results of freeze drying of HA/CHH NPs with TRE presented here are in
455 agreement with data obtained by de la Fuente et al. (2008), who did not observe significant
456 changes in the particle size after lyophilisation of HA/CHIT/tripolyphosphate NPs with either
457 5% w/v TRE or 5% w/v glucose. However, it needs to be highlighted that the concentrations
458 of NPs tested by de la Fuente et al. (2008) were lower (0.075-0.5 mg/ml) than those used
459 in this work. Also, no optimisation study on the concentration of cryoprotectant, nor tests
460 on the influence of NP composition on redispersibility were performed. As it is
461 demonstrated here, optimisation of the concentration of cryoprotectant is of vital
462 importance and the NP composition may have a significant influence on redispersibility,
463 with NPs containing higher amount of HA content requiring less TRE for stabilisation. Some
464 NP systems can be successfully redispersed even at the NP to cryoprotectant weight ratio of
465 1:1 (HA/CHH_{5;1} with 0.1% w/v TRE).

466 It is generally accepted that TRE is a more effective cryo-/lyo-protectant than
467 mannitol (Cegnar et al., 2011; Katas et al., 2013; Rampino et al., 2013). In contrast to
468 mannitol, TRE was an amorphous excipient after the process and yielded the most suitable
469 protective properties (Cegnar et al., 2011). Briefly, stabilisation of materials in sugar glasses
470 has been explained by the formation of a glassy sugar matrix, which acts as a physical
471 barrier between the particles and inhibits the diffusion on a relevant time scale (Allison et
472 al., 2000; Hafner et al., 2011; Molina et al., 2004). Sugar molecules isolate individual
473 particles in the unfrozen fraction, thereby preventing aggregation during freezing (Allison et
474 al., 2000; Rampino et al., 2013). The sugar molecule interact with NPs via hydrogen bonding,
475 maintaining them in the 'pseudo-hydrated state' during the dehydration step and replace
476 water, thus providing protection from damage during dehydration and subsequent
477 rehydration (Cegnar et al., 2011; Hirsjärvi et al., 2009; Rampino et al., 2013). Summarising
478 the outcomes of studies on HA/CHH NPs, lower TRE concentrations were needed for
479 formulations with lower NP concentrations in the native dispersions and higher HA/CHH
480 MMRs (more negative ZP) to successfully preserve NP properties post-processing.

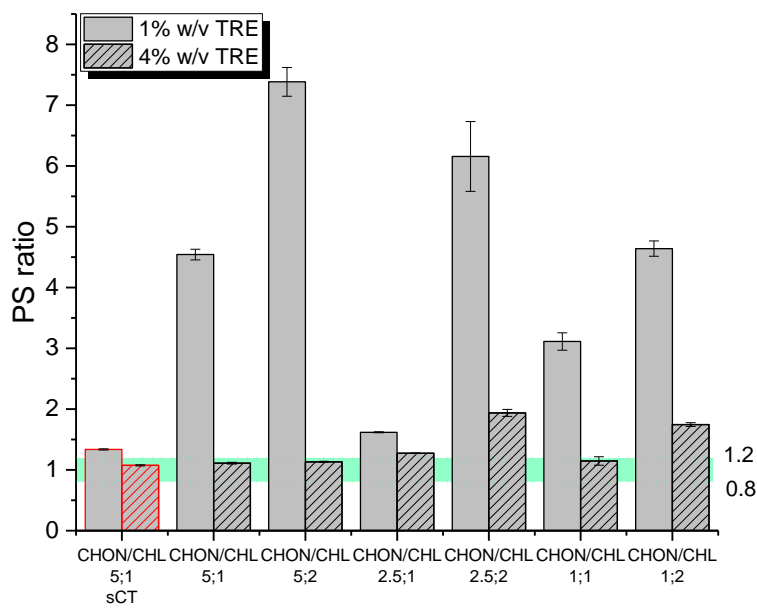
481 **3.2.3.2. CHON- and PROT-based NPs**

482 All HA/PROT NPs tested were successfully redispersed when freeze dried with 4%
 483 w/v TRE. The PS ratios after and before freeze drying were not significantly higher than 1.2
 484 (Figure 3a) and no aggregation was observed in any of the samples tested. When TRE
 485 concentration was decreased to 1% w/v, no aggregation was observed, but a slight increase
 486 in the particle size by 27, 34 and 27% was seen for the following samples: HA/PROT_{2.1;low},
 487 HA/PROT_{6.3;high} and HA/PROT_{3.1;high}, respectively. Therefore, even at 1% w/v TRE, acceptable
 488 or very good redispersion was observed depending on the composition of the sample for all
 489 HA/PROT NPs tested. However, the results show that HA/PROT NPs redisperse better than
 490 HA/CHH NPs with an MMR of 2.5 and 1.



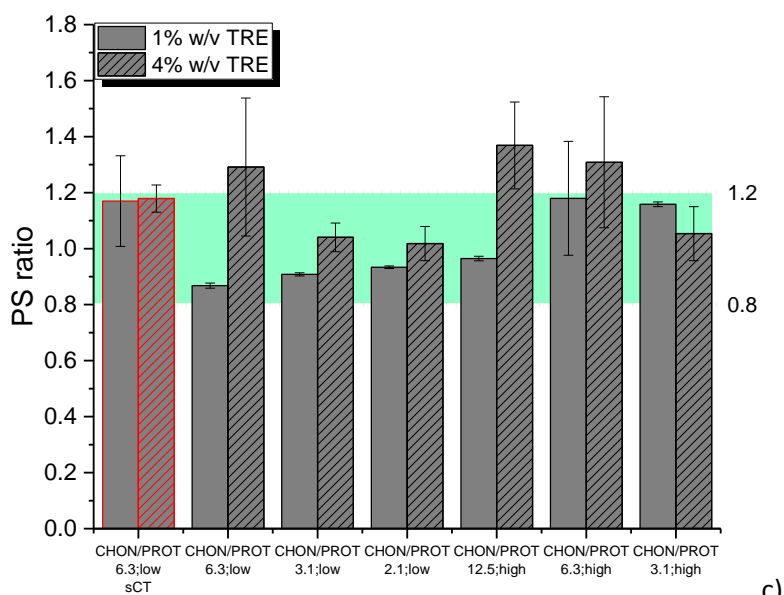
491

a)



492

b)



c)

493

494 **Figure 3.** The particle size (PS) ratio of: a) HA/PROT NPs, b) CHON/CHL NPs and c)
 495 CHON/PROT freeze dried with 1 and 4% w/v of TRE. The green bands indicate the PS ratio
 496 between 0.8 and 1.2, considered as very good redispersibility of processed NPs.

497

498

499 The redispersibility of CHON-based NPs was also examined in order to verify, if the
 500 polyanion (CHON versus HA) has any influence on reconstitution of NPs. As shown in Figure
 501 3b, none of the formulations tested were successfully redispersed after lyophilisation with
 502 1% w/v TRE. When the concentration of TRE was increased to 4% w/v, all formulations with
 503 the CHON/CHL MMR of 5 as well as CHON/CHL_{1,1} redispersed with a very good preservation
 504 of the particle size. In two formulations with a TPC of 2 mg/ml: CHON/CHL_{1,2} and
 505 CHON/CHL_{2.5,2}, aggregation was observed and the particle size was significantly increased
 506 after the process. Freeze dried CHON/CHL_{2.5,1} satisfactorily redispersed after processing with
 507 4% w/v TRE, but an increase in the particle size by 27% was observed.

508 The results obtained for CHON/CHL NPs confirm that the composition of the
 509 particles, especially the MMR of the polymers, and their concentration plays an important
 510 role affecting the ability of such NPs to be redispersed. Similarly to HA/CHH NPs, CHON/CHL
 511 NPs with a MMR of 2.5 were the most problematic in reconstitution studies and CHON/CHL
 512 NPs with a MMR of 5 were the easiest to fully reconstitute. Therefore, CHON/CHL NPs were
 513 characterised by worse redispersibility compared to HA-based NPs.

514 Finally, CHON/PROT NPs were freeze dried with 1 or 4% w/v TRE, and the results are
 515 shown in Figure 3c. Similarly to HA/PROT NPs, no aggregation was observed in any of the
 516 samples tested, and all samples satisfactorily redispersed even after processing with 1% w/v

517 TRE. In some samples an increase in the particle size by 30% could be observed, but they did
518 not differ significantly ($p>0.05$) from the PS ratio of 1.2. Interestingly, some of the NPs
519 freeze dried with 4% w/v TRE were significantly ($p<0.05$) larger than those lyophilised with
520 1% w/v TRE. The CHON /PROT_{12.5;high} system as well as all NPs made using 0.7 mg/ml CHON
521 decreased their size during freeze drying with 1% w/v TRE and the size ratios were smaller
522 than 1. In conclusion, both HA/PROT and CHON/PROT NPs are characterised by very good
523 redispersibility, which is considerably better than most of the chitosan-based formulations.

524 Differences in redispersibility of the NPs can possibly be explained by different
525 properties of the polyelectrolytes used (molecular weight, charge sign, charge strength and
526 charge density) and different NP structures. PROT has the highest charge density, CHON and
527 CHIT have low charge density, while the charge density of HA is very low. Strong
528 polyelectrolyte complexes are generally formed between polymers including anions and
529 cations of strong acids or bases in their structure (Denuziere et al., 1996). In contrast, weak
530 polyelectrolyte complexes are formed between weak acids and bases. CHIT contains
531 primary amine groups that are weak bases and PROT contains guanidinium groups that are
532 strong bases. HA has carboxylic groups (a weak acid), while CHON has both, sulphate (a
533 strong acid) and carboxylic groups. Therefore it is expected that, considering the pairs of
534 polyelectrolytes tested, CHIT forms with HA a weaker PEC than it does with CHON. Weaker
535 binding between HA and CHIT compared with that between CHON and CHIT can influence
536 the pore size and network complexity of particles and facilitate the penetration and
537 interactions with TRE, thereby improving redispersibility of the HA/CHIT PEC NPs. It has
538 been suggested that the PROT-based NPs do not show the core-corona structure (Umerska
539 et al., 2015, 2014b), in contrast to the CHIT-based NPs. If the dense, tightly packed core is
540 not formed in PROT-based NPs, it may facilitate the penetration of TRE into the NP structure
541 and interactions between TRE and NPs. In summary, it can be concluded that the NPs can be
542 ranked in terms of easiness of redispersibility as follows: HA/PROT > CHON/PROT >
543 CHON/CHL and that HA/CHH NPs reconstitute better in comparison to PROT- and CHON-
544 based NPs.

545 **3.2.4 Freeze drying of sCT-containing NPs with trehalose**

546 Having investigated freeze drying properties of HA/CHH carriers, sCT-loaded NPs
547 were freeze dried in the presence of TRE to study the impact of the peptide presence on
548 reconstitution and also the effect of processing on the peptide. The PS ratios are presented

549 in Figure 1 for HA/CHH_{5,1}sCT and in Figure 3 for PROT- and CHON-based systems. In relation
550 to HA/CHH_{5,1}sCT, although no aggregation was observed when the TRE concentration used
551 was in the range of 0.1-4%, a significant increase in the particle size after lyophilisation was
552 seen when lower concentrations of TRE were used. The particle size increased by 36, 63 and
553 83% when 0.5, 0.2 and 0.1% w/v of the sugar was used in the process, respectively.
554 Therefore the preservation of particle properties was not as good as for the equivalent
555 system with no sCT. Thus, incorporation of sCT decreases the ability of HA/CHH NPs to be
556 successfully redispersed. Nevertheless, it is noteworthy that even after increasing by 83% in
557 size the, particles still remained small with sizes well below 400 nm. No impact of sCT
558 loading was seen for the HA/PROT NPs. In contrast to HA-based NPs, incorporation of sCT
559 into CHON-based NPs (system CHON/CHL_{5,1}sCT) improved their redispersibility compared to
560 the equivalent carrier systems with no peptide loaded (CHON/CHL_{5,1}) (Figure 3). Despite the
561 fact that the sCT presence worsened redispersibility of HA-based NPs and enhanced
562 redispersibility of CHON-based NPs, HA/CHH/sCT NPs can be considered as easier to
563 redisperse than CHON/CHL/sCT NPs, because after freeze drying with 1% w/v TRE their
564 particle size was better maintained.

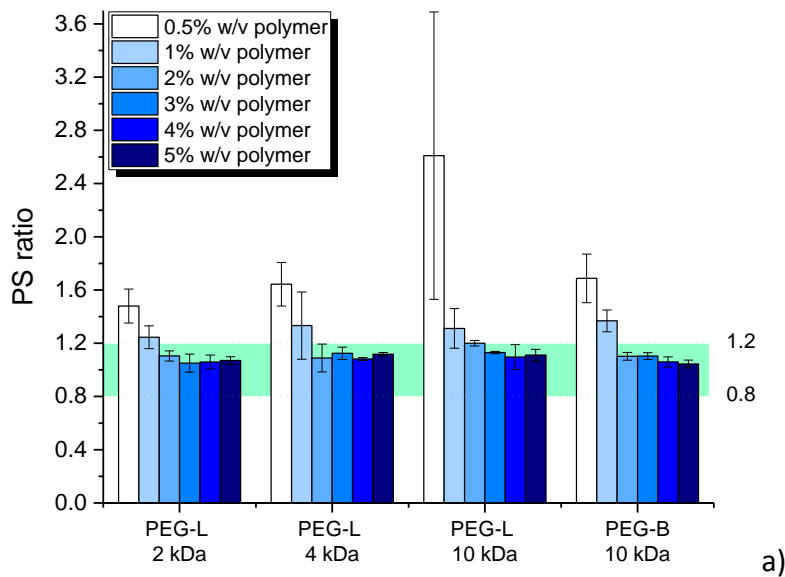
565 To confirm that no degradation of sCT occurred during the process, separation of
566 non-associated sCT in the reconstituted sample (HA/CHH_{5,1}sCT) by the previously described
567 ultrafiltration-centrifugation technique (Umerska et al., 2014a) was conducted. The amount
568 of peptide extracted from HA/CHH_{5,1}sCT after lyophilisation was 98.90±1.57%, compared to
569 96.80±2.19% for the sample before freeze drying used here as control. The association
570 efficiency (AE) was 98.92±0.28% and 98.94±0.27% before after processing, respectively,
571 indicating no impact of lyophilisation on the integrity of sCT. Also, when trying to maximise
572 the drug loading in the particles, the concentration of a cryoprotectant must be kept as low
573 as possible. The sCT loading in samples (HA/CHH) lyophilised with 0.1, 0.2, 0.5 and 1% w/v
574 TRE would be approximately 20, 14, 7.7 and 4.3% w/w, respectively, which can be
575 considered as high. However, a compromise must be made between the preservation of
576 properties of the particles and the drug loading.

577 In conclusion, the presence of sCT in the studied PEC NPs, with exception of the
578 HA/PROT system, affected the properties of NPs post-processing, but in an inconsistent
579 manner thus, if a cargo molecule is incorporated into PEC NPs it is likely that the optimum
580 cryoprotectant concentration will be different to that used for empty NP carriers.

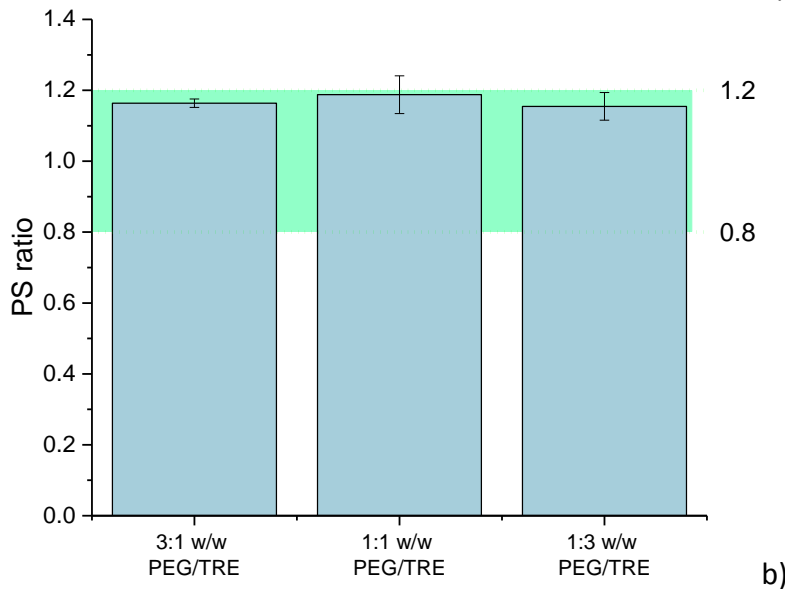
581 3.2.5. Freeze drying of HA/CHH NPs with PEG polymers

582 Apart from sugars, water soluble polymers could also be used as cryoprotectants.
583 Lee et al. (2009) have shown that 2000 g/mol PEG successfully performed as a
584 cryoprotectant for naproxen nano-suspensions. PEG chains in the crystal lattice are
585 organised as lamellae and the proportion of the crystal form is dictated by the molecular
586 weight of the polymer (Craig, 1995). As a consequence, PEG materials are semicrystalline
587 and may exhibit a significant degree of disorder (Craig, 1995). Therefore, in this part of the
588 study, HA/CHH_{2.5;1} with variable concentrations of different PEG polymers (2, 4 and 10 kDa
589 linear PEG as well as 10 kDa four-arm branched PEG). HA/CHH_{2.5;1} was poorly redispersible
590 when lyophilised with TRE (Figure 1).

591 Figure 4a shows the PS ratios after and before freeze drying of the systems with PEG
592 polymers. When 0.5% w/v PEG was used, aggregation was observed during reconstitution,
593 regardless of the type of PEG used. An increase in the polymer concentration to 1% w/v
594 resulted in an acceptable redispersibility of NPs with no aggregation observed and PS ratios
595 between 1.25 ± 0.09 and 1.37 ± 0.08 (for PEG 2 kDa and branched PEG 10 kDa, respectively). A
596 further increase in PEG concentration from 2 to 5% w/v led to very good redispersibility of
597 the systems with an increase in particle size after freeze drying smaller than 20%. Neither
598 the molecular weight nor the structure of PEG molecules (linear versus branched) were
599 found to have an impact on redispersibility of HA/CHH NPs. Also, PEG was found to be a
600 more effective cryoprotectant than TRE, as only 1% w/v PEG was needed to obtain
601 acceptable redispersibility of HA/CHH_{2.5;1} compared to 3% w/v TRE, where only marginal
602 redispersion was seen. Very good preservation of the size of NPs was achieved at 2% w/v
603 PEG compared to 4% w/v TRE.



604



605

606 **Figure 4.** The particle size (PS) ratio of HA/CHH_{2.5;1} freeze dried with: a) different
 607 concentrations of PEG polymers and b) 2% w/v solutions containing different proportions of
 608 PEG-L 2 kDa and TRE. The green bands indicate the PS ratio between 0.8 and 1.2, considered
 609 as very good redispersibility of processed NPs.
 610

611 3.2.6 Freeze drying of HA/CHH NPs with a mixture of trehalose and PEG

612 As PEG was shown to be a more effective cryoprotectant than TRE, attempts were
 613 made to decrease the concentration of the sugar required for the successful redispersion of
 614 HA/CHH_{2.5;1} after freeze drying with a mixture of cryoprotectants: TRE and PEG. Also, it was
 615 of interest if a combination of these two excipients may have a synergistic effect. As it has
 616 been shown that viscosity of aqueous PEG solutions increases proportionally to an
 617 increasing molecular weight (Gonzalez-Tello et al., 1994), therefore PEG with the lowest
 618 molecular weight (i.e. 2 kDa) was selected for further co-lyophilisation studies with TRE. The

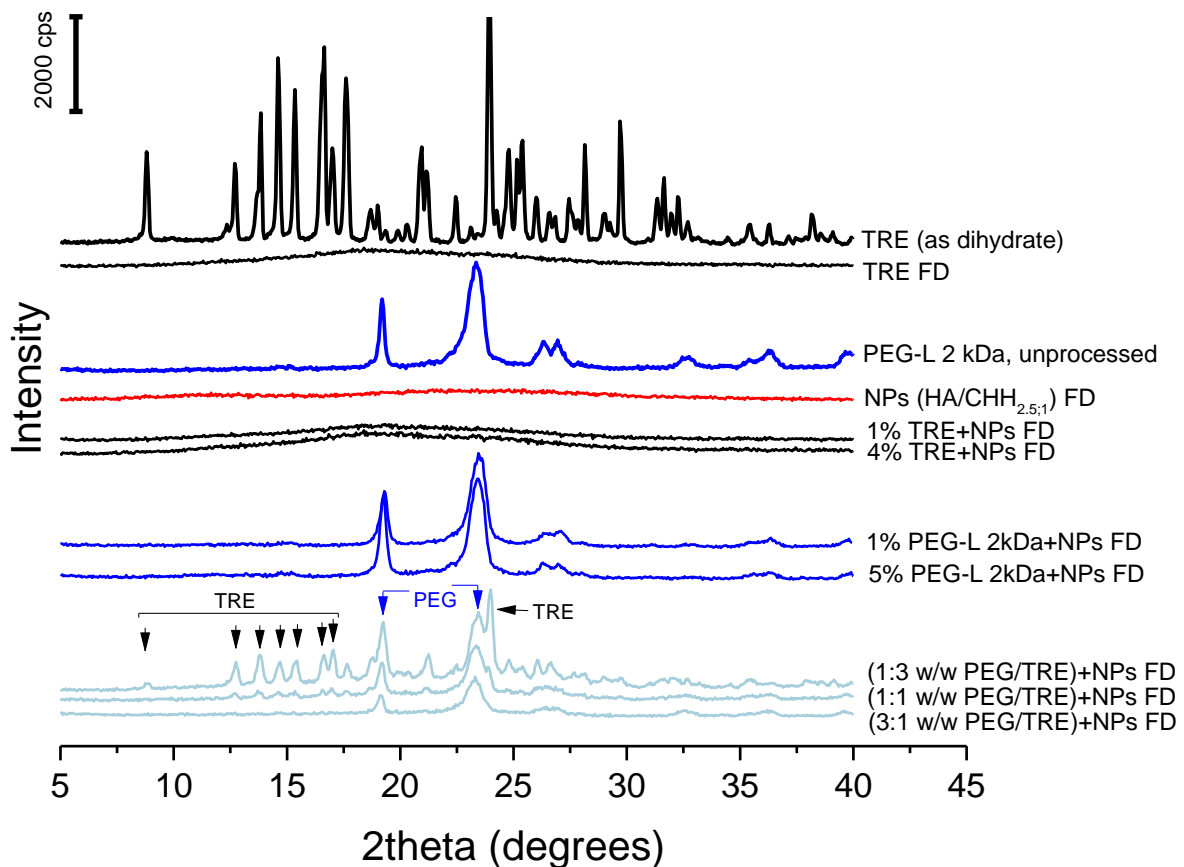
619 total concentration of cryoprotectants was kept at 2% w/v, and three combinations were
620 tested: 3:1, 1:1 and 1:3 w/w of PEG/TRE.

621 As shown in Figure 4b, the PS ratio was below 1.2 for all three combinations. More
622 importantly, aggregation was not observed. In relation to the synergistic effect of both
623 cryoprotectants when used in a combination, this was clearly seen for the 1:1 and 1:3 w/w
624 PEG/TRE mixtures, where the measured PS ratios were 1.19 ± 0.05 and 1.155 ± 0.04 , while
625 those calculated (theoretical) PS ratio values are 1.42 and 1.57, respectively. Therefore it
626 can be concluded, that addition of PEG enabled to decrease the concentration of TRE
627 required to successfully reconstitute freeze dried HA/CHH_{2.5;1} and that a synergistic effect of
628 the excipient combination was observed.

629 3.3. Solid state analysis of the freeze dried products

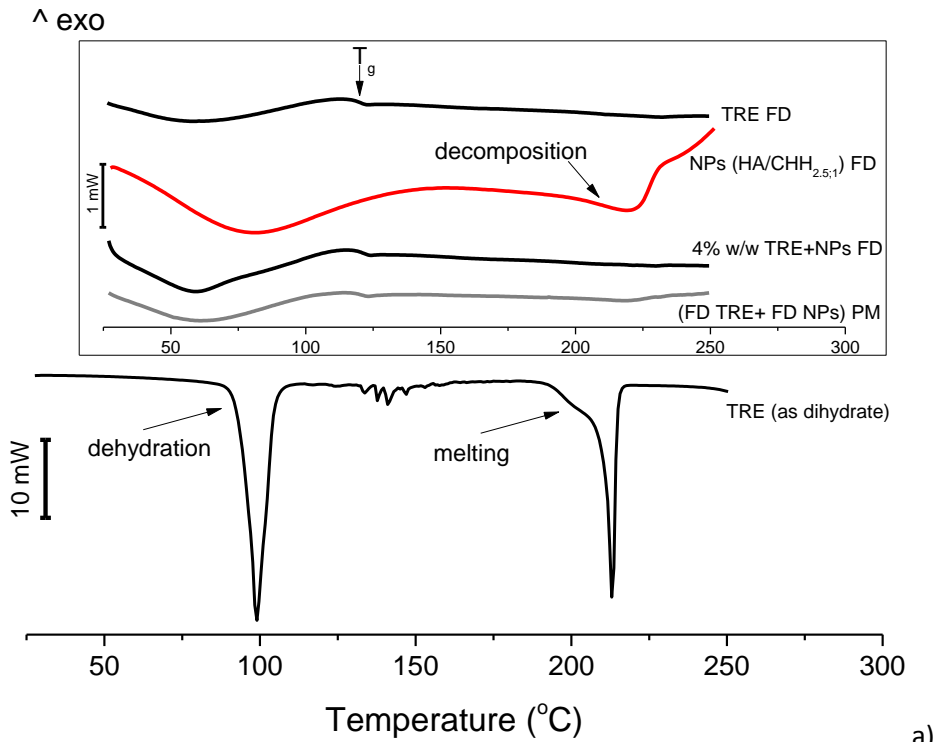
630 3.3.1. Trehalose/NPs systems

631 The NPs (HA/CHH_{2.5;1}) freeze dried without any cryoprotectant were PXRD
632 amorphous (Figure 5) and no clear thermal events, with exception of a shallow peak of
633 thermal decomposition after 200 °C, were observed in the DSC scans (Figure 6a).

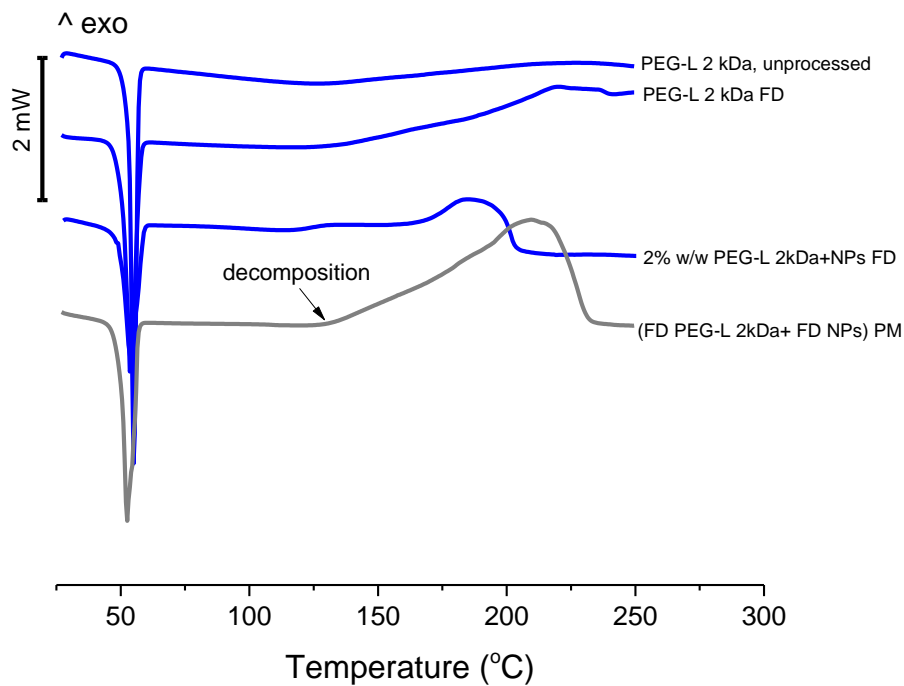


634 **Figure 5.** Powder X-ray diffractograms of (from top to bottom): unprocessed TRE as
635 trehalose dihydrate, freeze dried TRE (TRE FD), unprocessed PEG-L 2 kDa, freeze dried
636

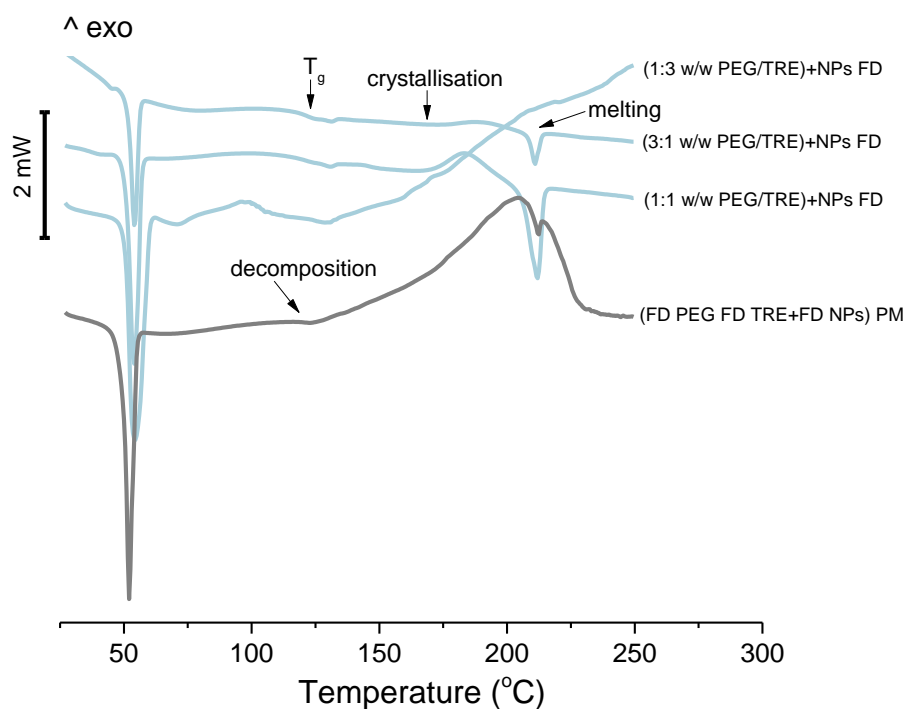
637 HA/CHH_{2.5:1} (referred to as NPs), NPs freeze dried in 1% w/v TRE (1% TRE+NPs FD), NPs
 638 freeze dried in 4% w/v TRE (4% TRE+NPs FD), NPs freeze dried in 1% w/v PEG-L 2 kDa (1%
 639 PEG-L 2kDa+NPs FD), NPs freeze dried in 5% w/v PEG-L 2 kDa (5% PEG-L 2kDa+NPs FD), NPs
 640 freeze dried in 2% w/v solution of 1:3 w/w PEG-L 2 kDa/TRE mixture ((1:3 w/w PEG/TRE)
 641 +NPs FD), NPs freeze dried in 2% w/v solution of 1:1 w/w PEG-L 2 kDa/TRE mixture ((1:1
 642 w/w PEG/TRE) +NPs FD), NPs freeze dried in 2% w/v solution of 3:1 w/w PEG-L 2 kDa/TRE
 643 mixture ((3:1 w/w PEG/TRE) +NPs FD). Arrows indicate characteristic diffraction peaks of
 644 trehalose dihydrate and PEG-L 2 kDa.
 645



646 a)



647 b)



648

649 **Figure 6.** Differential calorimetry thermograms of: a) unprocessed TRE as trehalose
 650 dihydrate, freeze dried TRE (TRE FD), freeze dried HA/CHH_{2.5;1} (referred to as NPs), NPs
 651 freeze dried in 4% w/v TRE (4% w/w TRE+NPs FD) and a physical mixture of TRE and NPs
 652 freeze dried separately ((FD TRE+ FD NPs) PM); b) unprocessed PEG-L 2 kDa, freeze dried
 653 PEG-L 2 kDa (PEG-L 2 kDa FD), NPs freeze dried in 2% w/v PEG-L 2 kDa (2% w/w PEG-L
 654 2kDa+NPs FD) and a physical mixture of PEG-L 2 kDa and NPs freeze dried separately ((FD
 655 PEG-L 2kDa+ FD NPs) PM); c) NPs freeze dried in 2% w/v solution of 3:1 w/w PEG-L 2
 656 kDa/TRE mixture ((3:1 w/w PEG/TRE)+NPs FD), NPs freeze dried in 2% w/v solution of 1:1
 657 w/w PEG-L 2 kDa/TRE mixture ((1:1 w/w PEG/TRE)+NPs FD), NPs freeze dried in 2% w/v
 658 solution of 1:3 w/w PEG-L 2 kDa/TRE mixture and a physical mixture of TRE ((1:3 w/w
 659 PEG/TRE)+NPs FD), PEG-L 2 kDa and NPs freeze dried separately ((FD PEG FD TRE+FD NPs)
 660 PM).

661

662 PXRD studies showed that initially crystalline, unprocessed trehalose dihydrate
 663 became amorphous after lyophilisation of its aqueous solution (Figure 5). It can be seen that
 664 the presence of NPs did not affect the solid state properties of freeze dried TRE. As shown in
 665 Figure 6a dehydration of trehalose dihydrate starting material powder occurs at 97.7 °C and
 666 the anhydrous crystals melt at 211.5 °C, consistent with temperatures of 97 and 210 °C,
 667 respectively, reported by Ohtake et al. (2011). The thermogram of lyophilised TRE (Figure
 668 6a) had a glass transition (T_g) of 119.3 °C, in agreement with the T_g of 110-120 °C recorded
 669 by Ohtake et al. (2011). After freeze drying HA/CHH_{2.5;1} with TRE, the T_g with a similar
 670 midpoint (120.5 °C) was observed, confirming that the sugar was amorphous (Figure 6a). No
 671 crystallisation exotherm was recorded, showing that the presence of NPs did not destabilise

672 the structure of amorphous TRE and furthermore, no visible NP decomposition event (at
673 around 200 °C) was noted, in contrast to the equivalent physical mixture composed of
674 HA/CHH_{2.5;1} and TRE freeze dried separately, indicating improved thermal stability of NPs
675 lyophilised with TRE.

676 **3.3.2. PEG/NPs systems**

677 PXR (Figure 5) and DSC (Figure 6b) show that unprocessed PEG-L 2 kDa was
678 crystalline. A narrow endotherm with an onset at 52.8°C and peak at 54.3°C was recorded
679 by DSC. After freeze drying PEG was crystalline, but the onset and peak of melting
680 endotherm appeared at lower temperatures (49.4 and 52.8 °C, respectively) and the
681 endotherm was broader compared to the unprocessed material. This may be a result of PEG
682 conformation change. PEG has a helical conformation consisting of seven chemical units and
683 two turns in a fibre identity period of 19.3 Å (Craig, 1995). On melting solid PEG, the helical
684 structure is lost and a liquid containing random coils is obtained. In aqueous solution the
685 system retains the helical configuration, but in a less ordered form (Craig, 1995). It is
686 possible that due to the rapid decrease in temperature, which takes place during freezing
687 aqueous solution of PEG with the use of liquid nitrogen before the lyophilisation process,
688 some chain conformation changes occur which affect the thermal behaviour of lyophilised
689 PEG.

690 The crystalline character of PEG was evident after freeze drying with HA/CHH_{2.5;1}. All
691 peaks present in the PXR diffractograms of the PEG/NP systems were similar to PEG on its
692 own and no extra peaks were seen indicating that no new phase was formed (Figure 5). As
693 HA/CHH_{2.5;1} did not show any clear thermal events, the endotherms seen in the DSC
694 thermograms of all PEG/NP systems could be attributed to the melting of PEG (Figure 6b).
695 These endothermic peaks were broader than that of the unprocessed PEG and the onsets
696 occurred at lower temperatures however, as the onset temperature for these systems was
697 around 49.6-49.7 °C, this shows mostly the effect of processing on PEG and not interactions
698 NPs-polymer. Again, the thermal stability of NPs in the lyophilisates was improved, as
699 thermal decomposition of the physical mixture of separately freeze dried HA/CHH_{2.5;1} and
700 PEG starts at 120 °C (Figure 6b).

701 **3.3.3. PEG/trehalose/NPs systems**

702 PXR (Figure 5) presented that lyophilisation of HA/CHH_{2.5;1} with all PEG-L 2 kDa/TRE
703 mixtures tested resulted in the formation of crystalline materials. The peaks characteristic of

704 PEG at approximately 19 and 23 2theta degrees were seen in all PEG/TRE/NPs
705 diffractograms. TRE on its own is amorphous after lyophilisation, however, a clear presence
706 of crystalline trehalose dihydrate was noticed in the freeze dried (1:1 w/w PEG/TRE)/NP
707 system and these peaks were more pronounced for the freeze dried (1:3 w/w PEG/TRE)/NP
708 sample. Hence the ratio of PEG to TRE dictates whether the sugar after freeze drying is
709 amorphous or crystalline.

710 DSC scans (Figure 6c) show the thermal characteristics of PEG/TRE/NPs. In all
711 thermograms an endotherm at approximately 50-55 °C is seen, which can be attributed to
712 melting of PEG. A clear T_g in DSC traces of (1:1 w/w PEG/TRE)/NPs and (1:3 w/w
713 PEG/TRE)/NPs is seen at approximately 120 °C, indicating of the presence of amorphous TRE
714 (also evident from PXRD data, Figure 5), thus these materials are semi-crystalline. This T_g is
715 comparable to that of pure, lyophilised TRE, thus suggesting no miscibility of PEG and TRE.
716 Crystallisation and melting of TRE is visible in the thermograms of (1:1 w/w PEG/TRE)/NPs
717 and (1:3 w/w PEG/TRE)/NP (Figure 6c). A crystallisation exotherm with an onset at 170-175
718 °C is immediately followed by an endotherm appearing at 205-208 °C for both samples. A
719 small endotherm of TRE melting was also present in the physical mix (TRE and PEG were
720 lyophilised separately), overlapping with an event of thermal degradation of sample.

721 The enthalpy of crystallisation of the (1:1 w/w PEG/TRE)/NPs system was 33 J/g,
722 while that for the (1:3 w/w PEG/TRE)/NPs sample was only 11 J/g, consistent with PXRD
723 showing greater crystallinity of TRE in (1:3 w/w PEG/TRE)/NPs. Interestingly, as no
724 crystallisation was observed in freeze dried amorphous TRE, it appears that the sugar in (1:1
725 w/w PEG/TRE)/NPs and (1:3 w/w PEG/TRE)/NPs is present in an amorphous and also the
726 crystalline, dihydrate form and the crystalline content is driving the amorphous phase to
727 crystallise. The thermogram of (3:1 w/w PEG/TRE)/NPs showed primarily melting of the PEG
728 component, followed by thermal decomposition starting at around 120 °C.

729 Overall, all PEG/TRE/NPs freeze dried mixtures were semi-crystalline with an
730 evidence of crystalline PEG and trehalose dihydrate present, thus these powders can be
731 considered as being more physically stable than lyophilised TRE/NPs.

732 **3.4. Cytotoxicity of the freeze dried products**

733 **3.4.1 Trehalose-based samples**

734 Cytotoxicity of TRE was examined, as it would be present in all the freeze dried NP
735 samples tested. When using different concentration of the sugar alone, 4% w/v is able to

736 decrease the cell viability by 13%. TRE appeared to decrease the viability of Caco-2 cells only
 737 at concentrations higher than 2% w/v. It is probably due to the fact that the high
 738 concentration of sugar results in hyperosmolar solutions and thus may reduce cells viability
 739 unspecifically (Scherließ, 2011). The IC₅₀ of TRE was calculated to be 5.8% w/v.

740 Table 3 shows the cytotoxicity of HA/CHH NPs. At the concentration of 4% w/v,
 741 which is a concentration typically resulting in good redispersibility of practically all NPs
 742 investigated, TRE can be considered as non-toxic. Although significant, the decrease in cell
 743 viability caused by TRE is small (7% decrease in cell viability compared to control determined
 744 by flow cytometry and 13% by MTS assay). The toxicity (by MTS assay) of freeze dried
 745 formulations with the HA/CHH MMR of 1 were comparable to toxicity of pure TRE. On the
 746 other hand, the MTS assay showed that reconstituted NPs, previously processed with 4%
 747 w/v TRE, with the HA/CHH MMR of 5 (HA/CHH_{5;2} and HA/CHH_{5;1}) were significantly less toxic
 748 than 4% w/v solution of TRE. The MTS results agreed with those from the flow cytometry
 749 assay. Lyophilised HA/CHH_{5;1} and HA/CHH_{5;2} had the amount of viable cells (Annexin V and PI
 750 negative) at 90.7±0.5 and 86.35±1.2%, respectively, thus the HA/CHH_{5;1} was significantly
 751 less cytotoxic than the solution of trehalose on its own. Therefore, no toxic effects were
 752 observed after the incubation of cells with reconstituted NPs with the HA/CHH MMR of 5
 753 moreover, the presence of HA/CHH_{5;1} seemed to reduce significantly the cytotoxic effects of
 754 TRE. The HA/CHH MMR=1 systems (lyophilised with 4% w/v TRE) were the most toxic
 755 HA/CHH samples (Table 3). It was not possible to determine the cell viability by flow
 756 cytometry due to the presence of micro-sized aggregates, which caused analysis
 757 interference. Incorporation of sCT into HA/CHH NPs (system HA/CHH_{5;1}sCT) decreased the
 758 viability of cells only slightly (7% decrease by MTS and 9% by flow cytometry), but the
 759 difference was statistically significant when compared to equivalent NPs with no sCT (Table
 760 3).

761

762 **Table 3** Viability studies (MTS assay and flow cytometry) of Caco-2 cells treated for 72 hours
 763 with 4% w/v TRE solution or with reconstituted, HA-based NPs previously freeze dried with
 764 4% w/v TRE. N/D – not determined; * - p < 0.05 vs. control, ** - p < 0.05 vs. TRE, *** - p <
 765 0.05 vs. control and TRE

Sample	% of viable cells by MTS assay	% of viable cells by flow cytometry
Serum-free medium (control) – no TRE	100	91.3±2.7

added		
TRE	82.9±1.9*	84.2±2.2*
HA/CHH _{5;1}	96.6±5.3**	90.7±0.5**
HA/CHH _{5;2}	89.9±0.9***	86.35±1.2*
HA/CHH _{5;1} SCT	89.7±1.0***	81.05±4.6*
HA/CHH _{1;1}	80.0±8.6	N/D
HA/CHH _{1;2}	75.8±8.8	N/D
HA/PROT _{6.3;low} SCT	68.8±14.35*	80.35±2.0*
HA/PROT _{6.3;low}	65.6±13.0*	81.3±2.0*
HA/PROT _{3.1;low}	60.8±9.6***	80.3±1.1*
HA/PROT _{2.1;low}	54.15±4.7***	77.9±1.05***
HA/PROT _{12.5;high}	67.6±4.1***	81.8±0.7*
HA/PROT _{6.3;high}	64.2±2.3***	78.35±1.6***
HA/PROT _{3.1;high}	46.8±6.2***	75.35±4.5***

766

767 Cytotoxicity of HA/PROT NPs freeze dried with TRE is presented in Table 3. The
768 viability of Caco-2 cells was decreased markedly compared to control (serum-free medium).
769 As noted earlier for PROT (Umerska et al., 2014b), the MTS assay was more sensitive than
770 flow cytometry. The viability of cells decreased by approximately 10-15% compared to the
771 medium in the apoptosis assay and a 30-50% decrease in the proliferation of the cells was
772 observed by MTS assay. The lyophilised samples contained two ingredients which have been
773 shown to decrease the amount of living cells: PROT (Umerska et al., 2014b) and high
774 concentration of TRE. HA/PROT NPs freeze dried with TRE were markedly more toxic than
775 TRE alone, however their toxicity does not differ significantly from PROT at the same
776 concentration (Umerska et al., 2014b) and increases as the content of PROT in the
777 formulation increases.

778 Table 4 shows the effects of freeze dried CHON/CHIT formulations had on Caco-2
779 cells. All formulations tested were well tolerated by the cell line. The cytotoxicity of freeze
780 dried samples did not differ significantly from those of HA/CHH systems with equivalent
781 composition. Also, similar effects were observed: incubation with formulations containing
782 more CHON (higher MMRs) resulted in a higher % of viable cells and a significant increase in
783 the number of living cells (especially visible for CHON/CHL_{5;1}). Therefore, the presence of
784 CHON/CHL NPs also protect Caco-2 cells from the negative effects of osmotic stress caused
785 by TRE. In relation to lyophilised CHON/PROT NP formulations, the number of living cells
786 decreased by 20-35%, depending on the composition of the sample (Table 4). In conclusion,

787 CHON/PROT NPs lyophilised with TRE were generally better tolerated than those composed
 788 of HA and PROT. Also, they were less toxic than PROT on its own.

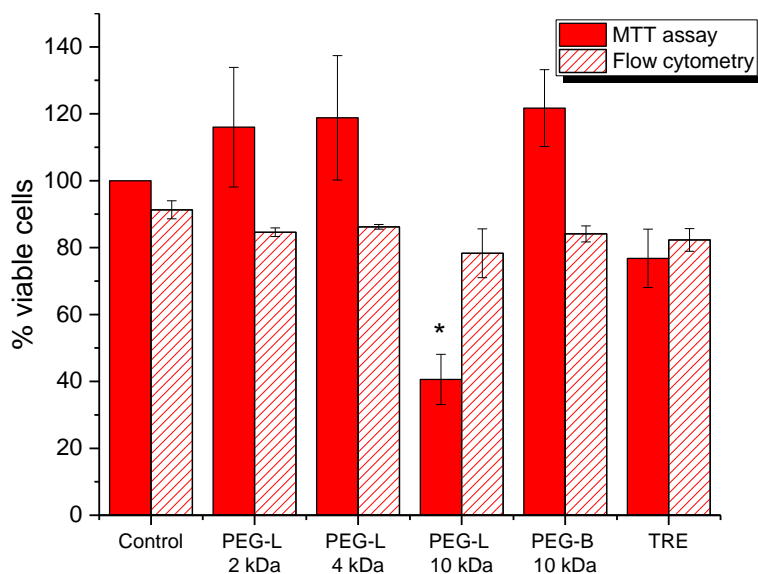
789 **Table 4** Viability (MTS assay) of Caco-2 cells by MTS assay treated for 72 hours with 4% w/v
 790 TRE solution or with reconstituted, CHON-based NPs, previously freeze dried with 4% w/v
 791 TRE. * - $p < 0.05$ vs. TRE

Sample	% of viable cells by MTS assay
TRE	82.9±1.9
CHON/CHL _{1;1}	79.6±8.3
CHON/CHL _{1;2}	84.4±11.2
CHON/CHL _{5;1}	98.4±7.9*
CHON/CHL _{5;2}	87.8±6.6
CHON/CHL _{5;1} SCT	86.0±8.7
CHON/PROT _{2.1;low}	72.2±14.1
CHON/PROT _{3.1;low}	74.8±5.9
CHON/PROT _{6.3;low}	80.2±5.2
CHON/PROT _{6.3;low} SCT	76.4±15.2
CHON/PROT _{3.1;high}	64.1±6.4*
CHON/PROT _{6.3;high}	74.05±11.4
CHON/PROT _{12.5;high}	75.3±5.4

792

793 3.4.1 PEG-based samples

794 Cytotoxicity of all PEG polymers (i.e. 2 kDa, 4 kDa, 10 kDa linear and 10 kDa branched
 795 PEG) was tested at the same concentration of 5% w/v by MTS assay and flow to compare
 796 their toxic effects. The results are shown in Figure 7. The PEG polymers, apart from 10 kDa
 797 linear PEG, were well tolerated by Caco-2 cells. MTS assay showed that the proliferation of
 798 cells was slightly increased after incubation with 2 and 4 kDa linear PEGs or 10 kDa branched
 799 PEG. A statistically significant decrease in the % of viable cells can be observed in the
 800 apoptosis assay for all these three polymer grades, however the viability was decreased by
 801 only approximately 5%. Interestingly, linear 10 kDa PEG decreased the viability of Caco-2
 802 cells significantly (40.6±7.5% of viable cells remained by MTS assay).



803
 804 **Figure 7.** Viability of Caco-2 cells after 72-hour exposure to solutions of different
 805 cryoprotectants at the concentration of 5% w/v. * - $p < 0.05$ vs control
 806

807 As the linear 10 kDa PEG was the most toxic from all cryoprotectants examined, the
 808 cytotoxicity of this PEG was also tested at lower concentrations. At 3 or 4% w/v linear 10
 809 kDa PEG remained toxic, however the detrimental effects were markedly reduced at 2% w/v
 810 and lower concentrations. The IC_{50} of 10 kDa linear PEG was 2.5% w/v, therefore it can be
 811 considered as more toxic than TRE.

812 4. Conclusion

813 A range of polyelectrolyte complex NPs were successfully obtained as solid state
 814 formulations with the employment of a lyophilisation process. The presence of a
 815 cryoprotectant was necessary to achieve a successful reconstitution and identified as a
 816 critical formulation parameter. Although freeze drying of PEC NPs was observed to be
 817 formulation specific, some general rules or guidelines on lyophilisation of such nanocarriers
 818 can be formulated based on the results obtained in this study:

819 1) NPs composed of a polycation and a polyanion that have a largely different
 820 molecular weight (here PROT-based NPs) are easier to redisperse than the NPs made of
 821 polymers with comparable molecular weight (here CHIT-based NPs).

822 2) NPs composed of weak polyelectrolytes with low charge density (HA) are easier to
 823 redisperse than NPs composed of strong polyelectrolytes with high charge density (CHON).
 824 Thus, NPs composed of weak polyelectrolytes are the preferred option if minimising
 825 cryoprotectant concentration is crucial to achieve satisfactory drug loading.

826 3) For a particular PEC pair the NPs that contain large stoichiometric excess of one of
827 the polymers are preferred because they are easier to redisperse. The particles with lower
828 crosslinking density are characterised by better redispersibility after freeze-drying because
829 of easier penetration of cryoprotectant molecules. Ionised active ingredients may affect the
830 redispersibility as they can modify crosslinking density.

831 4) If an active ingredient is incorporated into PEC NPs, it is likely that the minimal
832 cryoprotectant concentration required for successful redispersion will be different to that
833 used for empty NP carriers.

834 5) Low molecular weight compounds prone to quick crystallisation, such as mannitol,
835 should not be used as cryoprotectants in freeze drying of PEC NPs. Compounds that form an
836 amorphous state on lyophilisation, such as trehalose, are better candidates as
837 cryoprotectants for freeze drying of PEC NPs.

838 6) Non-charged polymers capable of forming multiple hydrogen bonds with PEC NPs
839 such as PEGs are more effective cryoprotectants than small molecular weight compounds.
840 However, there is no benefit in increasing the molecular weight of PEG and/or branching
841 and the linear 10 kDa PEG showed an increased toxicity.

842 7) Using a PEG/trehalose blend proved to be beneficial in terms of improved
843 redispersibility.

844 **5. Acknowledgements**

845 This study was funded by the Irish Drug Delivery Research Network, a Strategic
846 Research Cluster grant (07/SRC/B1154) under the National Development Plan co-funded by
847 EU Structural Funds and Science Foundation Ireland. This work was also supported by the
848 Synthesis and Solid State Pharmaceutical Centre funded by Science Foundation Ireland
849 under grant number 12/RC/2275. Author CM is SFI Stokes lecturer and author MJSM is an
850 Usher lecturer in Nanopharmaceutical Drug Discovery, Trinity College Dublin. Support from
851 Ireland's Higher Education Authority Programme for Research in Third Level Institutes (HEA
852 PRTL) Cycle 5 for the Trinity Biomedical Sciences Institute is also acknowledged.

853

854 **6. References**

855

- 856 Abdelwahed, W., Degobert, G., Stainmesse, S., Fessi, H., 2006. Freeze-drying of
857 nanoparticles: Formulation, process and storage considerations. *Adv. Drug Deliv. Rev.*
858 58, 1688–1713. <https://doi.org/10.1016/j.addr.2006.09.017>
- 859 Allison, S.D., Molina, M. d. C., Anchordoquy, T.J., 2000. Stabilization of lipid/DNA complexes
860 during the freezing step of the lyophilization process: The particle isolation hypothesis.
861 *Biochim. Biophys. Acta- Biomembr.* 1468, 127–138. [https://doi.org/10.1016/S0005-](https://doi.org/10.1016/S0005-2736(00)00251-0)
862 2736(00)00251-0
- 863 Anhorn, M.G., Mahler, H.C., Langer, K., 2008. Freeze drying of human serum albumin (HSA)
864 nanoparticles with different excipients. *Int. J. Pharm.* 363, 162–169.
865 <https://doi.org/10.1016/j.ijpharm.2008.07.004>
- 866 Boge, L., Västberg, A., Umerska, A., Bysell, H., Eriksson, J., Edwards, K., Millqvist-Fureby, A.,
867 Andersson, M., 2018. Freeze-dried and re-hydrated liquid crystalline nanoparticles
868 stabilized with disaccharides for drug-delivery of the plectasin derivative AP114
869 antimicrobial peptide. *J. Colloid Interface Sci.* 522, 126–135.
870 <https://doi.org/10.1016/j.jcis.2018.03.062>
- 871 Cegnar, M., Miklavžin, A., Kerč, J., 2011. Freeze-drying and release characteristics of
872 polyelectrolyte nanocarriers for the mucosal delivery of ovalbumin. *Acta Chim. Slov.* 58,
873 241–250.
- 874 Cesàro, A., De Giacomo, O., Sussich, F., 2008. Water interplay in trehalose polymorphism.
875 *Food Chem.* 106, 1318–1328. <https://doi.org/10.1016/j.foodchem.2007.01.082>
- 876 Craig, D.Q.M., 1995. A review of thermal methods used for the analysis of the crystal form,
877 solution thermodynamics and glass transition behaviour of polyethylene glycols.
878 *Thermochim. Acta* 248, 189–203. [https://doi.org/10.1016/0040-6031\(94\)01886-L](https://doi.org/10.1016/0040-6031(94)01886-L)
- 879 Crowe, L.M., Reid, D.S., Crowe, J.H., 1996. Is trehalose special for preserving dry
880 biomaterials? *Biophys. J.* 71, 2087–2093. [https://doi.org/10.1016/S0006-](https://doi.org/10.1016/S0006-3495(96)79407-9)
881 3495(96)79407-9
- 882 de la Fuente, M., Seijo, B., Alonso, M.J., 2008. Novel hyaluronan-based nanocarriers for
883 transmucosal delivery of macromolecules. *Macromol. Biosci.* 8, 441–450.
884 <https://doi.org/10.1002/mabi.200700190>
- 885 Denuziere, A., Ferrier, D., Domard, A., 1996. Chitosan-chondroitin sulfate and chitosan-
886 hyaluronate polyelectrolyte complexes. Physico-chemical aspects. *Carbohydr. Polym.*
887 29, 317–323. [https://doi.org/10.1016/S0144-8617\(96\)00035-5](https://doi.org/10.1016/S0144-8617(96)00035-5)
- 888 Fang, Z.G., Pan, P., Yang, Z.Q., Chen, Y.G., Zhang, J.K., Wei, M., Zhang, X.N., Zhang, Q., 2009.
889 Two Novel Freeze-Dried pH-Sensitive Cyclosporine A Nanoparticles: Preparation, in
890 vitro Drug Release, and in vivo Absorption Enhancement Effects. *Curr. Nanosci.* 5, 449–
891 456. <https://doi.org/10.2174/157341309789378140>
- 892 Gonzalez-Tello, P., Camacho, F., Blazquez, G., 1994. Density and Viscosity of Concentrated
893 Aqueous Solutions of Polyethylene Glycol. *J. Chem. Eng. Data* 39, 611–614.
894 <https://doi.org/10.1021/je00015a050>
- 895 Goutelle, S., Maurin, M., Rougier, F., Barbaut, X., Bourguignon, L., Ducher, M., Maire, P.,
896 2008. The Hill equation: A review of its capabilities in pharmacological modelling.
897 *Fundam. Clin. Pharmacol.* 22, 633–648. [https://doi.org/10.1111/j.1472-](https://doi.org/10.1111/j.1472-8206.2008.00633.x)
898 8206.2008.00633.x
- 899 Hafner, A., Dürriegl, M., Pepić, I., Filipović-Grčić, J., 2011. Short- and long-term stability of
900 lyophilised melatonin-loaded lecithin/chitosan nanoparticles. *Chem. Pharm. Bull.*

901 (Tokyo). 59, 1117–1123. <https://doi.org/10.1248/cpb.59.1117>

902 Hirsjärvi, S., Peltonen, L., Hirvonen, J., 2009. Effect of Sugars, Surfactant, and Tangential
903 Flow Filtration on the Freeze-Drying of Poly(lactic acid) Nanoparticles. *AAPS*
904 *PharmSciTech* 10, 488–494. <https://doi.org/10.1208/s12249-009-9236-z>

905 Holzer, M., Vogel, V., Mäntele, W., Schwartz, D., Haase, W., Langer, K., 2009. Physico-
906 chemical characterisation of PLGA nanoparticles after freeze-drying and storage. *Eur. J.*
907 *Pharm. Biopharm.* 72, 428–437. <https://doi.org/10.1016/j.ejpb.2009.02.002>

908 Iovu, M., Dumais, G., du Souich, P., 2008. Anti-inflammatory activity of chondroitin sulfate.
909 *Osteoarthr. Cartil.* 16, S14–S18. <https://doi.org/10.1016/j.joca.2008.06.008>

910 Jaques, L.B., 1973. Protamine-antagonist to heparin. *Can. Med. Assoc. J.* 108, 1291–1297.

911 Katas, H., Hussain, Z., Rahman, S.A., 2013. Storage stabilisation of albumin-loaded chitosan
912 nanoparticles by lyoprotectants. *Trop. J. Pharm. Res.* 12, 135–142.
913 <https://doi.org/10.4314/tjpr.v12i2.1>

914 Kim, A.I., Akers, M.J., Nail, S.L., 1998. The physical state of mannitol after freeze-drying:
915 Effects of mannitol concentration, freezing rate, and a noncrystallizing cosolute. *J.*
916 *Pharm. Sci.* 87, 931–935. <https://doi.org/10.1021/js980001d>

917 Liu, Z., Jiao, Y., Wang, Y., Zhou, C., Zhang, Z., 2008. Polysaccharides-based nanoparticles as
918 drug delivery systems. *Adv. Drug Deliv. Rev.* 60, 1650–1662.
919 <https://doi.org/10.1016/j.addr.2008.09.001>

920 Lu, X., Pikal, M.J., 2004. Freeze-Drying of Mannitol-Trehalose-Sodium Chloride-Based
921 Formulations: The Impact of Annealing on Dry Layer Resistance to Mass Transfer and
922 Cake Structure. *Pharm. Dev. Technol.* 9, 85–95. [https://doi.org/10.1081/PDT-](https://doi.org/10.1081/PDT-120027421)
923 [120027421](https://doi.org/10.1081/PDT-120027421)

924 Molina, M.D.C., Armstrong, T.K., Zhang, Y., Patel, M.M., Lentz, Y.K., Anchordoquy, T.J., 2004.
925 The stability of lyophilized lipid/DNA complexes during prolonged storage. *J. Pharm.*
926 *Sci.* 93, 2259–2273. <https://doi.org/10.1002/jps.20138>

927 Molpeceres, J., Aberturas, M.R., Chacón, M., Berges, L., Guzmán, M., 1997. Stability of
928 cyclosporine-loaded poly- Σ -caprolactone nanoparticles. *J. Microencapsul.* 14, 777–787.
929 <https://doi.org/10.3109/02652049709006828>

930 Peer, D., Florentin, A., Margalit, R., 2003. Hyaluronan is a key component in cryoprotection
931 and formulation of targeted unilamellar liposomes. *Biochim. Biophys. Acta - Biomembr.*
932 1612, 76–82. [https://doi.org/10.1016/S0005-2736\(03\)00106-8](https://doi.org/10.1016/S0005-2736(03)00106-8)

933 Platt, V.M., Szoka, F.C., 2008. Anticancer therapeutics: Targeting macromolecules and
934 nanocarriers to hyaluronan or CD44, a hyaluronan receptor. *Mol. Pharm.* 5, 474–486.
935 <https://doi.org/10.1021/mp800024g>

936 Quiñones, J.P., Peniche, H., Peniche, C., 2018. Chitosan based self-assembled nanoparticles
937 in drug delivery. *Polymers (Basel).* 10, 235. <https://doi.org/10.3390/polym10030235>

938 Raafat, D., Von Bargen, K., Haas, A., Sahl, H.G., 2008. Insights into the mode of action of
939 chitosan as an antibacterial compound. *Appl. Environ. Microbiol.* 74, 3764–3773.
940 <https://doi.org/10.1128/AEM.00453-08>

941 Rampino, A., Borgogna, M., Blasi, P., Bellich, B., Cesàro, A., 2013. Chitosan nanoparticles:
942 Preparation, size evolution and stability. *Int. J. Pharm.* 455, 219–228.
943 <https://doi.org/10.1016/j.ijpharm.2013.07.034>

944 Reynolds, F., Weissleder, R., Josephson, L., 2005. Protamine as an efficient membrane-
945 translocating peptide. *Bioconjug. Chem.* 16, 1240–1245.
946 <https://doi.org/10.1021/bc0501451>

947 Ryan, S.M., McMorrow, J., Umerska, A., Patel, H.B., Kornerup, K.N., Tajber, L., Murphy, E.P.,

948 Perretti, M., Corrigan, O.I., Brayden, D.J., 2013. An intra-articular salmon calcitonin-
949 based nanocomplex reduces experimental inflammatory arthritis. *J. Control. Release*
950 167, 120–129. <https://doi.org/10.1016/j.jconrel.2013.01.027>

951 Scherließ, R., 2011. The MTT assay as tool to evaluate and compare excipient toxicity in vitro
952 on respiratory epithelial cells. *Int. J. Pharm.* 411, 98–105.
953 <https://doi.org/10.1016/j.ijpharm.2011.03.053>

954 Shi, J., Votruba, A.R., Farokhzad, O.C., Langer, R., 2010. Nanotechnology in drug delivery and
955 tissue engineering: From discovery to applications. *Nano Lett.* 10, 3223–3230.
956 <https://doi.org/10.1021/nl102184c>

957 Tadros, T., 2010. General Principles of Colloid Stability and the Role of Surface Forces, in:
958 *Colloids and Interface Science Series*. pp. 1–22.
959 <https://doi.org/10.1002/9783527631193.ch1>

960 Umerska, A., Corrigan, O.I., Tajber, L., 2017. Design of chondroitin sulfate-based
961 polyelectrolyte nanoplexes: Formation of nanocarriers with chitosan and a case study
962 of salmon calcitonin. *Carbohydr. Polym.* 156, 276–284.
963 <https://doi.org/10.1016/j.carbpol.2016.09.035>

964 Umerska, A., Corrigan, O.I., Tajber, L., 2014a. Intermolecular interactions between salmon
965 calcitonin, hyaluronate, and chitosan and their impact on the process of formation and
966 properties of peptide-loaded nanoparticles. *Int. J. Pharm.* 477, 102–112.
967 <https://doi.org/10.1016/j.ijpharm.2014.10.023>

968 Umerska, A., Gaucher, C., Oyarzun-Ampuero, F., Fries-Raeth, I., Colin, F., Villamizar-
969 Sarmiento, M.G., Maincent, P., Sapin-Minet, A., 2018. Polymeric nanoparticles for
970 increasing oral bioavailability of Curcumin. *Antioxidants* 7, E46.
971 <https://doi.org/10.3390/antiox7040046>

972 Umerska, A., Paluch, K.J., Inkielewicz-Stepniak, I., Santos-Martinez, M.J., Corrigan, O.I.,
973 Medina, C., Tajber, L., 2012. Exploring the assembly process and properties of novel
974 crosslinker-free hyaluronate-based polyelectrolyte complex nanocarriers. *Int. J. Pharm.*
975 436, 75–87. <https://doi.org/10.1016/j.ijpharm.2012.07.011>

976 Umerska, A., Paluch, K.J., Martinez, M.J.S., Corrigan, O.I., Medina, C., Tajber, L., 2014b. Self-
977 assembled hyaluronate/protamine polyelectrolyte nanoplexes: Synthesis, stability,
978 biocompatibility and potential use as peptide carriers. *J. Biomed. Nanotechnol.* 10,
979 3658–3673. <https://doi.org/10.1166/jbn.2014.1878>

980 Umerska, A., Paluch, K.J., Santos-Martinez, M.J., Medina, C., Corrigan, O.I., Tajber, L., 2015.
981 Chondroitin-based nanoplexes as peptide delivery systems - Investigations into the self-
982 assembly process, solid-state and extended release characteristics. *Eur. J. Pharm.*
983 *Biopharm.* 93, 242–253. <https://doi.org/10.1016/j.ejpb.2015.04.006>

984 Veilleux, D., Gopalakrishna Panicker, R.K., Chevrier, A., Biniecki, K., Lavertu, M., Buschmann,
985 M.D., 2018. Lyophilisation and concentration of chitosan/siRNA polyplexes: Influence
986 of buffer composition, oligonucleotide sequence, and hyaluronic acid coating. *J. Colloid*
987 *Interface Sci.* 512, 335–345. <https://doi.org/10.1016/j.jcis.2017.09.084>

988 Wong, J.J.L., Yu, H., Hadinoto, K., 2018. Examining practical feasibility of amorphous
989 curcumin-chitosan nanoparticle complex as solubility enhancement strategy of
990 curcumin: Scaled-up production, dry powder transformation, and long-term physical
991 stability. *Colloids Surfaces A Physicochem. Eng. Asp.* 537, 36–43.
992 <https://doi.org/10.1016/j.colsurfa.2017.10.004>

993 Yang, J., Han, S., Zheng, H., Dong, H., Liu, J., 2015. Preparation and application of
994 micro/nanoparticles based on natural polysaccharides. *Carbohydr. Polym.* 123, 53–66.

995
996

<https://doi.org/10.1016/j.carbpol.2015.01.029>